Enhancing the Performance of Downlink NOMA Relaying Networks by RF Energy Harvesting and Data Buffering at Relay

Nguyen Nhu Thang
Dai hoc Ky thuat Le Quy Don
Tran Manh Hoang
Dai hoc Ky thuat Le Quy Don
Ba Cao Nguyen
Dai hoc Ky thuat Le Quy Don
Phuong T. Tran (tranthanhphuong@tdtu.edu.vn)
Ton Duc Thang University https://orcid.org/0000-0002-1448-8882

Research

Keywords: NOMA, energy harvesting, successive interference cancellation, power allocation, buffer-aided

Posted Date: December 3rd, 2020

DOI: https://doi.org/10.21203/rs.3.rs-117143/v1

RESEARCH

Enhancing the performance of downlink NOMA relaying networks by RF energy harvesting and data buffering at relay

Nguyen Nhu Thang[1], Tran Manh Hoang[1], Ba Cao Nguyen[1] and Phuong T. Tran[2*]

*Correspondence: tranthanhphuong@tdtu.edu.vn
[2]Wireless Communications Research Group, Faculty of Electrical and Electronics Engineering, Ton Duc Thang University., Ho Chi Minh City, Vietnam
Full list of author information is available at the end of the article

Abstract

Recently, non-orthogonal multiple access (NOMA) has been considered as a promising candidate for next-generation mobile communications because it can significantly improve the spectral efficiency of wireless networks. In this paper, we investigate a novel solution to enhance the reliability and the supply stability of a downlink NOMA relaying networks, in which we integrate two techniques: (i) simultaneous wireless information and power transfer, i.e. the relay node can harvest the energy from source signals and use this energy to help forward information from source node to two user nodes; and (ii) data buffer aid at relay node, i.e. the data packets received from the source can be stored in a buffer and then be re-transmitted to the destination nodes only when the channel condition is good. The performance of the proposed system is analyzed rigorously to derive the system outage probability and the average packet delay. Furthermore, a power allocation optimization problem to minimize the outage probability is formulated and solution to this problem is also provided in this paper. Monte Carlo simulations are conducted to verify the analytical results, which confirms that with the data buffer at the relay, the overall outage probability (OOP) has been reduced significantly.

Keywords: NOMA; energy harvesting; successive interference cancellation; power allocation; buffer-aided

Introduction

The non-orthogonal multiple-access (NOMA) is considered as a promising multiuser communication technique for the fifth-generation (5G) mobile network since it can achieve superior spectral efficiency [1]. Unlike the orthogonal-multiple-access (OMA), NOMA users can share the same radio resources, including time and bandwidth. The key idea for this advantage is to employ the power domain or codes domain, where different users are distinguished by their power levels or different code[2]. Recent researcher have shown that NOMA can be applied to not only point-to-point but also relay networks [3]. While the application of NOMA to the point-to-point networks were well investigated, there are still increasing needs for the case of cooperative relaying networks [4, 5]. The work in [4] studied the conventional cooperative NOMA system with buffer-aided relaying. Under the assumption that the relay node possesses a buffer. Herein the authors considered an adaptive transmission scheme in which different working modes are employed in different time slots. The authors of [5] proposed a dual-hop cooperative relaying scheme using NOMA, where two source nodes communicate with each other simultaneously via a common relay on the same frequency band. In this scheme, after receiving symbols transmitted in parallel by both sources with different power levels, the relay forwards the superposition coded composite signal using NOMA to two destinations. However, in this work power control for uplink multiple access was not considered.

In addition, harvesting energy from the ambient environment has become a promising solution for energy-constrained electronic devices, which are conventionally supported by limited power sources such as battery [6, 7, 8, 9]. In some special applications, charging the battery is too expensive or even impossible, e.g. sensor network works under toxic environment and body area network. Moreover, some natural energy sources such as solar and wind, and radio frequency (RF) can be also utilized as effective sources for energy harvesting (EH). Compared with other kinds of energy sources, the RF energy harvesting [10], also known as wireless energy transfer, has some advantages. Since the RF energy harvesting is an active energy supply method, it can provide more reliable energy flow to guarantee the quality of service.

Therefore, utilizing RF-EH technique together with NOMA scheme helps prolong the lifetime and improves the spectral utilization efficiency of the energy-constrained multi-user wireless relaying networks. The NOMA systems combining with RF energy harvesting is investigated in [11, 12, 13, 14]. A simultaneous wireless information and power transfer (SWIPT) of NOMA networks were considered in [11], where base station serves two types of users, namely, relay user and far user. The outage performance and spectral efficiency of the NOMA-EH relaying networks with antenna selection were investigated in [13], where the power splitting (PS) protocol is applied at the relay to harvest the energy. In [13], the performance of NOMA system is also compared with OMA system. The authors of [14] investigated a NOMA system in which NOMA users near to the source act as the EH relays to assist the far NOMA users in forwarding the information. In these works, the authors considered the users reception signals in two different time slots, however, the service was simultaneously provided to users in the NOMA system. The impact of power allocation in the cooperative NOMA network with SWIPT was investigated in [3]. In this work, Yang et. al. proposed two types of NOMA power allocation policies, namely NOMA with fixed power allocation (F-NOMA) and cognitive radio inspired NOMA (CR-NOMA). The results of these above-mentioned works shown that the performance of NOMA outperform OMA scheme. However, the diversity gain was not improved.

An energy buffer-aided EH relay was applied in cooperative communication system to improve sytem performance in [15], but in this work the authors didn't consider buffer-aided data. On the other hand, the work in [16] proposed a hybrid NOMA/OMA system with buffer-aided relay selection. As a result, two buffer-aided opportunistic relay selection algorithms were proposed. The aim of that work is to improve the outage performance and sum-rate of the system.

The authors in [17] proposed a priority-based max-link relay selection for data-buffer-aided decode-and-forward DF cooperative networks. In this work, the authors derived analytical expressions of outage probability and bit error rate to evaluate the system performance. In addition to NOMA downlink system investigation, the hybrid NOMA/OMA uplink system with the help of a buffer-aided relay was also considered in [18].

So far, all previous works related to cooperative communication protocols and NOMA technique in literature have proposed the superposition signal coding at the source. Meanwhile, the relay node, which has a fixed power, only decodes and forwards signals to destinations. However, due to the random nature of wireless channel, the amount of energy harvested at the relay is usually very small and variable. Hence, the power allocation at the relay can reduce the feedback energy and guarantee the performance fairness for all users. To the best of our knowledge, combining SWIPT with NOMA relaying system where the buffer-aided relay technique is employed at the relay has not been investigated in literature and the derivation of the overall outage probability expression of this system has not been carried out, either. Motivated by these facts, in this paper, we proposed a different cooperative decode-and-forward relaying scheme where a source transmits information packets to the relay, while relay broadcasts the modulation superposition signals to two users. However, R employs time switching based EH prior to the communication with destinations. Based on the channel gain from the relay node to the destination node, the relay performs fixed and optimal power allocation for two users. Furthermore, NOMA technology is investigated for the cooperative transmission in term of two scenarios, i.e. with and without buffer aid at the relay node.

The main contributions of this paper are summarized as below:

- We proposed a novel downlink NOMA relay system applying SWIPT, where designated relay node is either equipped with buffer or not. To harvest energy, the relay uses time switching protocol. The performance of the system is improved, and additionally the spectral utilization efficiency and the lifetime of wireless networks will be enhanced.
- The optimal power allocation at the relay node to minimum outage probability is also considered in this paper. Since the harvested energy is very small, the reallocation of the harvested energy after converting from the RF signals of the source is important for saving cost.
- Markov chain model and state-transition matrix is used to describe the random process at the buffer-aided relay. On the other hand, with buffer-aided relay the diversity gain is improved significantly.
- The system performance is demonstrated by the outage probability and the sum end-to-end ergodic capacity over Rayleigh fading channel. We derive the closed-form expression to evaluate the rate of symbols and outage performance of NOMA-SWIPT system.
- The analytical results are validated by simulation. From the derived closed-form expressions, practical networks can be investigated in the in future.

Our proposed system can be applied in surveillance sensor networks for disaster detection or Internet of Things (IoT), where installing fixed power lines or frequenty replacing the batteries for a large number of nodes is not convenient. Besides, its advantages such as low energy cost, reducing greenhouse effect, and prolonging timelife are useful for future mobile networks.

The remaining of the paper is organized as follows. Section "System model" presents the NOMA-SWIPT system model and channel model. The analysis of outage probability with and without buffer aid at the relay node is given in Sections "Outage probability without buffer-aided relay" and "Analysis of the outage probability with buffer-aided relay", respectively. The average packet delay is demonstrated in Section "Average packet delay of the buffer-aided relay system". Numerical results, which verify our analysis, are presented in Section "Numerical results". Finally, the conclusion is given in Section "Conclusion".

For the convenience, we provide in Table 1 the notations along with their descriptions used in this paper.

Table 1 Mathematical notations

Notation	Description
$\Pr$	Probability
$F_X(x)$	Cumulative distribution function (CDF)
$f_X(x)$	Probability density function (PDF)
$\mathcal{CN}(\mu,\sigma^2)$	A circularly symmetric complex Gaussian RV x with mean μ and variance σ^2
$\mathbb{E}\{\cdot\}$	The statistical expectation operator
$\Gamma(\cdot)$	Gamma function [27]
$\mathcal{K}_n(\cdot)$	The second kind of Bessel function order n[27]
$\mathrm{E}_n(z)$	Exponential integral function n[27]
$G_{pq}^{mn}(x\|_{b_s}^{a_r})$	Meijer's G-Function [27, 9.3]

Methods

System model

The system model of a NOMA downlink relaying network investigated in this paper is shown in Fig 1. According to this model, a source (S) wants to send its messages to two destinations (D_1) and (D_2) simultaneously with the help of relay node, (R), which is capable of energy harvesting. It is assumed that S, D_1, and D_2 have fixed power supply while relay node have no extra embedded energy supply, hence, R needs to harvest energy from S. In addition, the relay node is assumed to have an unlimited-size information buffer to store the received messages [19]. We assume that the direct link between the source and destination is not available due to far distance or deep shadow fading in the channel. All nodes are equipped with a single antenna and operate in a half-duplex mode[1].

The channels between two arbitrary nodes are subject to block and flat Rayleigh fading. This means that the channel coefficients are constant during each data block transmission interval T but vary from one block to another.

In the case that the relay uses a buffer for data processing, we assume that it has perfect channel state information (CSI) of the links $\mathrm{S} \rightarrow \mathrm{R}$ and $\mathrm{D}_1, \mathrm{D}_2 \rightarrow \mathrm{R}$ at the beginning of each time slot by using a short reference signals. Based on this set of information, R can decide whether it is ready to operate in transmitting or receiving mode [20].

As shown in Fig. 1, the complex channel coefficient of the link between S and R is denoted by $h_1 \sim \mathcal{CN}\left(0, \Omega_0\right)$. The complex channel coefficient between R and D_i, is $g_i \sim \mathcal{CN}\left(0, \Omega_i\right)$, where $i = \{1, 2\}$ and $\Omega_1 = \mathbb{E}\{|g_1|^2\}, \Omega_2 = \mathbb{E}\{|g_2|^2\}$. The additive white Gaussian noise (AWGN) at R, D_1 and D_2 is respectively denoted by $\mathrm{w}_{\mathcal{A}} \sim \mathcal{CN}\left(0, \mathrm{N}_0\right)$, where $\mathcal{A} \in \{\mathrm{R}, \mathrm{D}_1, \mathrm{D}_2\}$. Without loss of generality, we assume that the users' channel gains are sorted in the descending order as follows: $\left|g_1\right|^2 > \left|g_2\right|^2$.

Data buffer at relay

In order to process the data the relay is equipped with a buffer for storing the signals received from the source. For time switching (TS) scheme the relay also has an energy storage device to store the harvested energy[2]. R first harvests the energy from the RF signal transmitted by S and then performs signal reception and transmission using the harvestet and transmit strategy [21].

The system operates according to the time-division duplex (TDD) mode where each transmission period is divided into equal time slots of length $\tau(1-\alpha)$. At each time slot, the relay or source node is selected to transmit data depending on the status of the relay buffers and the available links that can provide the successful transmission or reception of one packet.

---

[1] This model can employ two antennas for the relay node and operate in a full-duplex mode.

[2] The storing of harvested energy in TS scheme is refered as charging-then-communicate. In contrast, PS scheme is refered as charging-and-communicate.

If S is selected, it will generate a transmission frame of size $2r_0\tau$ bits, intended for two destination nodes D_1 and D_2, to send to the relay node, where r_0 is the target transmission rate of the system. Each frame contains two segments, the first one is used for transmission symbols to D_1 and the second one is used for transmission symbols to D_2. The relay buffer has $L \geq 2$ storage units, each can store $2r_0\tau(1-\alpha)$ bits. The relay node decodes the received frame and stores it into the storage device. Each storage device is split into two parts of the same length, which are used to store the information symbols intended for D_1 and D_2, respectively.

Signal model

In each time slot, if the source is selected to transmit with unicast communication, it combines two signals x_1 and x_2 into a transmission packet. Then, the received signal at the relay is given by

$$y_{\mathrm{R}} = h_1\sqrt{P_{\mathrm{S}}}x_S + w_{\mathrm{R}}. \quad (1)$$

The signal-to-noise ratio (SNR) of the source-to-relay link is given by [19]

$$\gamma_{\mathrm{R}} = \frac{P_{\mathrm{S}}|h_1|^2}{N_0}. \quad (2)$$

The time switching (TS) architecture for harvesting energy is applied as [22]. Refer to [22] for more detailed explanation[3].

Herein, T denote the block duration of an entire communication period in which the information is transmitted from S to $\mathrm{D_i}$. For each period T, the first amount of time, αT, is used for EH at R, while the remaining amount of time, $(1-\alpha)T$, is used for transmiting and receiving the information, where α denotes the EH time fraction in one transmission block and $0 \leq \alpha \leq 1$. Therefore, the amount of harvested energy at the relay for the case of linear model in the ith time slot is given by [24, 25]

$$E_h = \alpha T \eta P_{\mathrm{S}}|h_1|^2, \quad (3)$$

[3] The proposed analytical approach can be applied to the power spitting EH model [23]

where η denotes the energy conversion efficiency whose value ranges from 0 to 1, depending on the harvesting electric circuitry.

Remark 1: In practice, the energy harvester will output a constant power because of the circuit design for EH-RF. The key of such a non-linear model is that it can capture the joint effect of the non-linear phenomena caused by hardware constraints including circuit sensitivity limitations and current leakage. The main cause of non-linear energy harvesting models can be mentioned by the relationship between the input RF power and the output direct current of energy harvester. The cause to make the nonlinear function can be explained by circuit devices such as diodes and transistors in the energy harvester structure. Denote P_{th} as the saturation power threshold of harvester, thus the transmit power of the relay node in proposed model of manuscript is given by

$$P_{\mathrm{R}} = \begin{cases} \frac{2\alpha\eta}{1-\alpha} P_{\mathrm{S}} |h_1|^2, \ P_{\mathrm{S}}|h_1|^2 \leq P_{\mathrm{th}} \\ \frac{2\alpha\eta}{1-\alpha} P_{\mathrm{th}}, \ P_{\mathrm{S}}|h_1|^2 > P_{\mathrm{th}}. \end{cases} .$$

.

We assume that all the amount of power harvested is consumed by the relay for forwarding signals to all users $\mathrm{D_i}$, the processing power for the transmitting/receiving circuitry at the relay is generally negligible compared to the power used for signal transmission and perhaps venial. So, from (3), the transmission power of the relay is given as

$$P_{\mathrm{R}} = \frac{E_h}{(1-\alpha)T/2} = \frac{2\alpha\eta P_{\mathrm{S}}|h_1|^2}{(1-\alpha)}. \tag{4}$$

In a specific time slot, if R is selected, it transmits a modulation superimposition information symbol $x_{\mathrm{R}} = \sqrt{a_1 P_{\mathrm{R}}} x_1 + \sqrt{(1-a_1)P_{\mathrm{R}}} x_2$ stored in the buffer through multicast communication, where x_1 and x_2 denote the information symbols intended for D_1 and D_2, respectively. a_1 is the power allocation coefficient for D_1. At the end of a time slot, the received signal at the destinations is given by

$$y_{\mathrm{D}_i} = \sqrt{P_{\mathrm{R}}} g_i (\sqrt{a_1} x_1 + \sqrt{1-a_1} x_2) + \mathrm{w}_{\mathrm{D}_i}. \tag{5}$$

When $|g_1|^2 > |g_2|^2$, according to the NOMA principle, the relay allocates more power for D_2, in order to balance the fairness of the system performance. Due to the broadcast nature of the wireless environment, we have the instantaneous signal-to-interference-and-noise ratio (SINR) of the $\mathrm{R} \to \mathrm{D}_2$ link given by

$$\gamma_{\mathrm{D}_2}^{x_2} = \frac{(1-a_1)P_{\mathrm{R}}|g_2|^2}{a_1 P_{\mathrm{R}}|g_2|^2 + N_0}, \tag{6}$$

where the information symbol x_1 is treated as the interference at D_2. At D_1, the goal is to decode information symbol x_1 of themselves. By applying the SIC principle[4], D_1 can remove the detected information symbol x_2 from the set of received signals. From (5), the instantaneous SNR and SINR of the $\mathrm{R} \to \mathrm{D}_1$ link is expressed as

$$\gamma_{\mathrm{D}_1}^{x_2 \to x_1} = \frac{(1-a_1)P_{\mathrm{R}}|g_1|^2}{a_1 P_{\mathrm{R}}|g_1|^2 + N_0}, \tag{7}$$

$$\gamma_{\mathrm{D}_1}^{x_1} = \frac{a_1 P_{\mathrm{R}}|g_1|^2}{N_0}. \tag{8}$$

Outage probability without buffer-aided relay

In this section, we investigate the outage performance of the SWIPT NOMA downlink relaying in two cases, i.e., the overall outage probability and the outage probability for each destination.

Overall outage probability

The overall outage probability (OOP) of the system is defined as the probability that neither the source-to-relay link nor the relay-to-both destinations links is unavailable for transmission to achieve the target predefined transmission rate. For simplicity, we assume that the target transmission rates from the source to the relay and the relay to the destinations are the same and equal to r_0. Hence, the instantaneous end-to-end capacity is $\frac{1-\alpha}{2}\log_2(1+\gamma_{\mathrm{e2e}}) < r_0$, and the outage event happens, the factor of $\frac{1-\alpha}{2}$ is due to the two consecutive time slots for communication between the source and the destination. Outage probability is equivalent to the probability that output SNR, γ_{e2e}, falls below a certain threshold, $\gamma_{\mathrm{th}} = 2^{\frac{2r_0}{1-\alpha}} - 1$.

The following theorem provides the exact closed-form expression of the overall outage probability and the approximation of the outage probability of the SWIPT-NOMA downlink relaying system.

---

[4] In this paper, we assume that the system is equipped with ideal successive interference cancellation (SIC) technique [26].

Theorem 1 *The overall outage probability of the system when the relay knows both g_1 and g_2 is given by*

$$\mathrm{OOP} = 1 - \frac{1}{\Omega_1}\sum_{k=0}^{\infty}\frac{(-1)^k}{k!}\left(\frac{\Psi_{\min}}{\Omega_2}\right)^k \times\left[\frac{(-1)^k}{(k-1)!}\left(\frac{1}{\Omega_1}\right)^{k-1}\mathrm{Ei}\left(\frac{-\gamma_{\mathrm{th}}}{\Omega_1 P_{\mathrm{S}}}\right)+\frac{\exp\left(\frac{-\gamma_{\mathrm{th}}}{\Omega_1 P_{\mathrm{S}}}\right)}{\left(\frac{\gamma_{\mathrm{th}}}{P_{\mathrm{S}}}\right)^{k-1}}\sum_{j=0}^{k-2}\frac{(-1)^j\left(\frac{\gamma_{\mathrm{th}}}{\Omega_1 P_{\mathrm{S}}}\right)^j}{\prod_{\ell=0}^{j}(k-1-\ell)}\right], \quad (9)$$

where $Ei(x)$ denotes the exponential integral function [27], $\phi = \frac{2\alpha\eta}{1-\alpha}$, $\Psi_{\min} = \min\left\{\frac{\gamma_{\mathrm{th}}}{a_1\phi P_{\mathrm{S}}}, \frac{\gamma_{\mathrm{th}}}{\phi P_{\mathrm{S}}(1-a_1(1+\gamma_{\mathrm{th}}))}\right\}$, and the condition $a_1 < \frac{1}{1+\gamma_{\mathrm{th}}}$ holds.

At high SNR regime, the approximation of OOP *is given by*

$$\mathrm{OOP} \approx 1 - \exp\left(-\frac{\gamma_{\mathrm{th}}}{\Omega_1 P_{\mathrm{S}}}\right) - \sqrt{\frac{4\Psi_{\min}}{\Omega_1\Omega_2}}\mathcal{K}_1\left(\sqrt{\frac{4\Psi_{\min}}{\Omega_1\Omega_2}}\right), \quad (10)$$

where $\mathcal{K}_1(\cdot)$ is the first-order modified Bessel function of the second kind.

Proof Please refer to Appendix A. When the condition $a_1 < \frac{1}{1+\gamma_{\mathrm{th}}}$ holds, which means the overall outage probability does not occur, we need to allocate more power to D_2. With assumption that SIC information symbol x_2 at the D_1 is perfect, if the relay knows the channel responses g_1 and g_2, it can adjust the power allocation coefficient a_1 to balance the outage probability of the relay-to-destinations links.

It should be noted that if $|g_1|^2 > |g_2|^2$, we have

$$\frac{(1-a_1)P_{\mathrm{R}}|g_1|^2}{a_1 P_{\mathrm{R}}|g_1|^2 + N_0} > \frac{(1-a_1)P_{\mathrm{R}}|g_2|^2}{a_1 P_{\mathrm{R}}|g_2|^2 + N_0}. \quad (11)$$

This remark is very important for analyzing the outage probability expressions in the next part. ■

Outage probability at the destination

In this section, we derive a closed-form expression of the outage probability at each destination. When one destination is in outage, the other can detect its corresponding information symbol. The system may switch to the conventional OMA system. However, in this case, the system performance will be degraded because the total power of the relay have been fixed division for D_1 and D_2.

Theorem 2 provides closed-form expressions of outage probabilities at D_1 and D_2, respectively.

Theorem 2 *The outage probability at* D_1 *and* D_2 *are given respectively in* (12) *and* (13) *below*

$$\mathrm{OP}_{\mathrm{D}_1} = 1 - \frac{1}{\Omega_1}\sum_{t=0}^{\infty}\frac{(-1)^t}{t!}\left(\frac{\mathcal{Q}_{\max}}{\Omega_2}\right)^t \times\left[\frac{(-1)^t}{(t-1)!}\left(\frac{1}{\Omega_1}\right)^{t-1}\mathrm{Ei}\left(\frac{-\xi_1}{\Omega_1 P_{\mathrm{S}}}\right) + \frac{\exp\left(\frac{-\xi_1}{\Omega_1 P_{\mathrm{S}}}\right)}{\left(\frac{\xi_1}{P_{\mathrm{S}}}\right)^{t-1}}\sum_{k=0}^{t-2}\frac{(-1)^k\left(\frac{1}{\Omega_1}\right)^k\left(\frac{\xi_1}{P_S}\right)^k}{\prod_{\ell=0}^{k}(t-1-\ell)}\right], \tag{12}$$

$$\mathrm{OP}_{\mathrm{D}_2} = 1 - \frac{1}{\Omega_1}\sum_{m=0}^{\infty}\frac{(-1)^m}{m!}\left(\frac{b}{\Omega_2}\right)^m \left[\frac{(-1)^m}{(m-1)!}\left(\frac{1}{\Omega_1}\right)^{m-1}\mathrm{Ei}\left(\frac{-\xi_2}{\Omega_1 P_{\mathrm{S}}}\right) + \frac{\exp\left(\frac{-\xi_2}{\Omega_1 P_{\mathrm{S}}}\right)}{\left(\frac{\xi_2}{P_{\mathrm{S}}}\right)^{m-1}}\sum_{q=0}^{m-2}\frac{(-1)^q\left(\frac{1}{\Omega_1}\right)^q\left(\frac{\xi_2}{P_{\mathrm{S}}}\right)^q}{\prod_{v=0}^{q}(m-1-v)}\right]. \tag{13}$$

where $\mathcal{Q}_{\max} = \max\left\{\frac{\xi_1}{a_1\phi P_{\mathrm{S}}}, \frac{\xi_1}{\phi P_{\mathrm{S}}(1-a_1(1+\xi_1))}\right\}$, $b = \frac{\xi_2}{\phi P_{\mathrm{S}}(1-a_1(1+\xi_2))}$, $\xi_1 = 2^{\frac{2r_1}{1-\alpha}} - 1$, $\xi_2 = 2^{\frac{2r_2}{1-\alpha}} - 1$, *and the condition* $a_1 \leq \frac{1}{1+\xi_i}$, $i \in \{1,2\}$ *holds.* r_1 *and* r_2 *are the target transmission rates at* D_1 *and* D_2*, respectively.*

Proof To obtain the outage probability expression of D_1 and D_2, we first analyze the instantaneous SINR and SNR of D_1 and D_2. It should be noted that in order to prove this theorem we assume that $|g_1|^2 > |g_2|^2$. Please refer to Appendix B. ■

Optimal power allocation to minimize the outage probability

In this section, we study the power allocation problem to minimize the outage probability of the EH-NOMA system.

Theorem 3 *The optimal power allocation coefficient* a_1^* *to minimize the outage probability in the EH-NOMA system is given by*

$$a_1^* = \frac{1}{2+\gamma_{\mathrm{th}}}. \tag{14}$$

Proof To obtain the minimum OOP and minimum $\mathrm{OP}_{\mathrm{D}_1}$ in (9) and (12) we formulate the outage probability minimization problems P1 and P2 as follows:

$$\begin{aligned} \mathrm{P1} : & \min_{a_1} \ \mathrm{OOP}, \\ \text{s.t. } & 0 \le a_1 \le 1, & (15) \\ & a_1 < \frac{1}{1+\gamma_{\mathrm{th}}}. & (16) \end{aligned}$$

and

$$\begin{aligned} \mathrm{P}_2 : & \min_{a_1} \ \mathrm{OP}_{\mathrm{D}_1}, \\ \text{s.t. } & 0 \le a_1 \le 1, & (17) \\ & a_1 < \frac{1}{1+\xi_1}. & (18) \end{aligned}$$

The condition $a_1 < \frac{1}{1+\gamma_{\mathrm{th}}}$ indicates that the outage event does not occur, i.e., the outage probability is less than one. The problems P1 and P2 are equivalent to maximizing $\Psi_{\min} = \min\left\{\frac{\gamma_{\mathrm{th}}}{a_1\phi P_{\mathrm{S}}}, \frac{\gamma_{\mathrm{th}}}{\phi P_{\mathrm{S}}(1-a_1(1+\gamma_{\mathrm{th}}))}\right\}$ and $\mathcal{Q}_{\max} = \max\left\{\frac{\xi_1}{a_1\phi P_{\mathrm{S}}}, \frac{\xi_1}{\phi P_{\mathrm{S}}(1-a_1(1+\xi_1))}\right\}$. In addition, we assume that $\gamma_{\mathrm{th}} = \xi_1$, which means that the data rate of D_1 is equal to the system data rate.

$$\begin{aligned} \mathrm{P1} : & \max\left\{\min\left(\frac{1}{a_1}, \frac{1}{1-a_1(1+\gamma_{\mathrm{th}})}\right)\right\}, \\ \text{s.t. } & 0 \le a_1 \le 1, & (19) \\ & a_1 < \frac{1}{1+\gamma_{\mathrm{th}}}. & (20) \end{aligned}$$

$$\begin{aligned} \mathrm{P2} : & \max\left\{\max\left(\frac{1}{a_1}, \frac{1}{1-a_1(1+\gamma_{\mathrm{th}})}\right)\right\}, \\ \text{s.t. } & 0 \le a_1 \le 1, & (21) \\ & a_1 < \frac{1}{1+\gamma_{\mathrm{th}}}. & (22) \end{aligned}$$

We consider two cases of the objective functions P1 and P2 under the following conditions:

$$a_1^* = \left(\frac{1}{a_1} \le \frac{1}{1-a_1(1+\gamma_{\mathrm{th}})}\right) \cup \left(\frac{1}{a_1} \ge \frac{1}{1-a_1(1+\gamma_{\mathrm{th}})}\right). \tag{23}$$

These problems can be solved similarly as those in [28, 4.1].

After some mathematical manipulations, we obtain the optimal power allocation coefficient a_1^* as shown in Theorem (3). It should be noticed that the power allocation for D_1 is considered, subject to the condition that the outage probability of D_2 certaintly occurs[5]. ■

Analysis of the outage probability with buffer-aided relay

In this section, we investigate the outage probability of the system where the buffer aid is employed at the relay node. For convenience, we assume that the source node always has data to transmit. We also consider the number of transmitted symbols as the number of transmitted packets. The relay chooses a node to transmit (source or relay) in a given time slot. To perform this, the information of the outage states of the links $\mathrm{S} \to \mathrm{R}$ and $\mathrm{R} \to \mathrm{D}$ is required. Therefore, the system uses one bit for the feedback information from the destination to the relay. This information helps R known if the link $\mathrm{R} \to \mathrm{D}$ is in outage or not. One bit which feedbacks from the relay to source is used to control the source in the transmit or silent mode. The source transmits the packets to the relay. Then, the relay decodes the packets and stores the decoded packets in its buffer. After that, the relay transmits the packets to the destination node. If the source is selected to transmit but the link $\mathrm{S} \to \mathrm{R}$ is in outage, the source remains silent and the outage occurs. Similarly, if the relay is selected to transmit but the link $\mathrm{R} \to \mathrm{D}$ is in outage, the relay remains silent and the outage occurs. Therefore, the system performance will be improved with the help of a buffer-aided relay. Unlike the case of without a buffer-aided relay, in this case the outage event is defined as the probability that the relay does not receive and transmit. In other words, the relay remains silent. To describe the state transition of the buffer-aided relay, we denote the outage events of $\mathrm{S} \to \mathrm{R}$ link and $\mathrm{R} \to \mathrm{D}$ link by $\mathcal{O}_{\mathrm{SR}}$ and $\mathcal{O}_{\mathrm{RD}}$, respectively. When the links are not in outage, the probabilities are: $1 - \mathcal{O}_{\mathrm{SR}} = \bar{\mathcal{O}}_{\mathrm{SR}}$ and $1 - \mathcal{O}_{\mathrm{RD}} = \bar{\mathcal{O}}_{\mathrm{RD}}$, respectively. In addition, the relay decision scheme is described as in Table 2. In Table 2, 'SR' denotes the link from the source to the relay nodes, "RD" refers to the link from the relay to the destination nodes; 'l' and 'L' respectively represents the packets stored in the

---

[5] Moreover, if the relay knows the channel gains g_1 and g_2 and the total power factor $a_1 + a_2$ is equal to one, we can allocate power for D_1 and D_2 by adapting to channel gains, i.e. $a_1 = |g_2|^2/(|g_1|^2 + |g_2|^2)$, to ensure the fairness of the outage performance.

Table 2 The Relay Decision Scheme

Case	SR	RD	l	Relay	The outage
A	0	0		Silent	$\mathcal{O}_{\rm SR}\mathcal{O}_{\rm RD}$
B	0		$l=0$	Silent	$\mathcal{O}_{\rm SR}$
C		0	$l=L$	Silent	$\mathcal{O}_{\rm RD}$
D	1	0	$l<L$	Receive	$\bar{\mathcal{O}}_{\rm SR}\mathcal{O}_{\rm RD}$
E	0	1	$l>0$	Transmit	$\mathcal{O}_{\rm SR}\bar{\mathcal{O}}_{\rm RD}$
F	1	1	$l\geqslant 2$	Transmit	$\bar{\mathcal{O}}_{\rm SR}\bar{\mathcal{O}}_{\rm RD}$
G	1	1	$l\leqslant 1$	Receive	$\bar{\mathcal{O}}_{\rm SR}\bar{\mathcal{O}}_{\rm RD}$

buffer and the buffer size at the relay node. 'Relay' denotes the decision of the relay node (silent, receive or transmit), '$\mathcal{OP}$' is the outage probability of the considered system. It is noted that in Table 2, the outage and non-outage links are indicated by '0' and '1', respectively.

To calculate the $\mathcal{OP}$ of the system, from the Table 2, we build the Markov chain. We start at the initial state $l=0$ (i.e. when the buffer is empty). If the link SR is in outage which means the source does not transmit, then, the buffer will be empty. In other words, the buffer state moves from $l=0$ to $l=0$ with probability of $\mathcal{O}_{\rm SR}$ (Case B in Table 2). When the link SR is not in outage, we consider two cases. The first case is when the link RD is in outage (Case D). Consequently, the relay receives the signal, making the buffer state moves from $l=0$ to $l=1$ with probability of $(1-\mathcal{O}_{\rm SR})\mathcal{O}_{\rm RD}$. The second case is when the link RD is not in outage (Case G). The relay receives the signal, making the buffer state moves from $l=0$ to $l=1$ with probability of $(1-\mathcal{O}_{\rm SR})(1-\mathcal{O}_{\rm RD})$. Combining these two cases, the buffer state moves from $l=0$ to $l=1$ with probability of $1-\mathcal{O}_{\rm SR}$. Similarly, we can obtain the probability of moving to the next state. From here, we have the Markov chain showing the state transitions as depicted in Fig. 2. When the buffer is empty ($l=0$), it stays empty with probability of $\mathcal{O}_{\rm SR}$ (case B) and receives a packet with probability of $1-\mathcal{O}_{\rm SR}$ (case D, G). When the buffer has one packet ($l=1$), it stays in the current state with probability of $\mathcal{O}_{\rm SR}\mathcal{O}_{\rm RD}$ if the relay does not receive and transmit (case A). If the relay receives one packet, it moves to the new state ($l=2$) with probability of $1-\mathcal{O}_{\rm SR}$ (case D, G) and is back to the initial state ($l=0$) with probability of $\mathcal{O}_{\rm SR}(1-\mathcal{O}_{\rm RD})$ (case E). When the buffer has l packets ($2\leqslant l\leqslant L-1$), it stays in this state with probability of $\mathcal{O}_{\rm SR}\mathcal{O}_{\rm RD}$ (case A), receives one packet with probability of $(1-\mathcal{O}_{\mathrm{SR}})\mathcal{O}_{\mathrm{RD}}$ (case D), and transmits one packet with probability of $1-\mathcal{O}_{\mathrm{RD}}$ (case E, F). If the buffer is full, which means that it has L packets, it remains the same state with probability of $\mathcal{O}_{\mathrm{RD}}$ (case C) and transmits one packet with probability of $1-\mathcal{O}_{\mathrm{RD}}$ (case E, F).

From Table 2 and the presented Markov chain, the outage probability of the system is calculated as

$$\begin{aligned}\mathcal{OP} &= \mathcal{O}_{\mathrm{SR}}\Pr\{l=0\}+\mathcal{O}_{\mathrm{RD}}\Pr\{l=L\}\\ &\quad+\mathcal{O}_{\mathrm{SR}}\mathcal{O}_{\mathrm{RD}}(1-\Pr\{l=0\}-\Pr\{l=L\}),\end{aligned} \tag{24}$$

where $\Pr\{l=0\}$ and $\Pr\{l=L\}$ are the probabilities of the events that the buffer is empty and full, respectively. To derive the $\mathcal{OP}$ of the system in (24), we define a state transition matrix $\mathbf{A}$ with size of $(L+1)\times(L+1)$ of the Markov chain, where $\mathbf{A}_{ij}$ denotes the element of the ith row and jth column of the matrix $\mathbf{A}$. It should be reminded that $\mathbf{A}_{ij}$ refers to the probability of moving from state i at time t to state j at time $t+1$, i.e.,

$$\mathbf{A}_{ij}=\Pr\{l_{t+1}=j|l_t=i\}. \tag{25}$$

For the case of $L=5$, matrix $\mathbf{A}$ is expressed as follows

$$\mathbf{A}=\begin{pmatrix}\mathcal{O}_{\mathrm{SR}} & \bar{\mathcal{O}}_{\mathrm{SR}} & 0 & 0 & 0 & 0\\ \mathcal{O}_{\mathrm{SR}}\bar{\mathcal{O}}_{\mathrm{RD}} & \mathcal{O}_{\mathrm{SR}}\mathcal{O}_{\mathrm{RD}} & \bar{\mathcal{O}}_{\mathrm{SR}} & 0 & 0 & 0\\ 0 & \bar{\mathcal{O}}_{\mathrm{RD}} & \mathcal{O}_{\mathrm{SR}}\mathcal{O}_{\mathrm{RD}} & \bar{\mathcal{O}}_{\mathrm{SR}}\mathcal{O}_{\mathrm{RD}} & 0 & 0\\ 0 & 0 & \bar{\mathcal{O}}_{\mathrm{RD}} & \mathcal{O}_{\mathrm{SR}}\mathcal{O}_{\mathrm{RD}} & \bar{\mathcal{O}}_{\mathrm{SR}}\mathcal{O}_{\mathrm{RD}} & 0\\ 0 & 0 & 0 & \bar{\mathcal{O}}_{\mathrm{RD}} & \mathcal{O}_{\mathrm{SR}}\mathcal{O}_{\mathrm{RD}} & \bar{\mathcal{O}}_{\mathrm{SR}}\mathcal{O}_{\mathrm{RD}}\\ 0 & 0 & 0 & 0 & \bar{\mathcal{O}}_{\mathrm{RD}} & \mathcal{O}_{\mathrm{RD}}\end{pmatrix}. \tag{26}$$

We should note that matrix $\mathbf{A}$ is not symmetric because the states are not symmetric and the number of links to other states is not the same, leading to the transition probabilities are not the same. Then, the stationary distribution $\boldsymbol{\pi}$ of the Markov chain is expressed as

$$\boldsymbol{\pi}=(\mathbf{A}-\mathbf{I}+\mathbf{B})^{-1}\mathbf{b}, \tag{27}$$

where $\mathbf{I}$ is an identity matrix, $\mathbf{B}$ is an $(L+1)\times(L+1)$ matrix with all elements equal to 1, and $\mathbf{b}=(\ 1\quad 1\quad \ldots\quad 1\ )^T$.

Theorem 4 *With the buffer-aided relaying, the outage probability of the system becomes*

$$\mathcal{OP} = \sum_{i=1}^{L+1} \boldsymbol{\pi}_i \mathbf{A}_{ii}. \tag{28}$$

To determine the state transit matrix $\mathbf{A}$, we need to derive $\mathcal{O}_{\mathrm{SR}}$ and $\mathcal{O}_{\mathrm{RD}}$. We assume that the minimum data transmission rate from S $\rightarrow$ R is r_0, then the outage probability of S $\rightarrow$ R link is defined as follows

$$\mathcal{O}_{\mathrm{SR}} = \Pr\left(\frac{1-\alpha}{2}\log_2(1+\gamma_{\mathrm{R}}) < r_0\right) = 1 - \exp\left(-\frac{\gamma_{\mathrm{th}}}{\Omega_{\mathrm{SR}} P_{\mathrm{S}}}\right). \tag{29}$$

According to the SIC principle, if D_1 is able to remove x_2 from its received signal, the outage probability of the link from the relay to the destinations nodes is given by

$$\mathcal{O}_{\mathrm{RD}} = \Pr\left(\frac{1-\alpha}{2}\log_2\left(1+\max\left\{\gamma_{\mathrm{D}_1}^{x_1}, \gamma_{\mathrm{D}_2}^{x_2}\right\}\right) < r_0\right). \tag{30}$$

After some manipulations, we have

$$\begin{aligned}\mathcal{O}_{\mathrm{RD}} = 1 &- \sqrt{\frac{4\mathcal{A}}{\Omega_{\mathrm{SR}}}} K_1\left(\sqrt{\frac{4\mathcal{A}}{\Omega_{\mathrm{SR}}}}\right) - \sqrt{\frac{4\mathcal{B}}{\Omega_{\mathrm{SR}}}} K_1\left(\sqrt{\frac{4\mathcal{B}}{\Omega_{\mathrm{SR}}}}\right) \\ &+ \sqrt{\frac{4(\mathcal{A}+\mathcal{B})}{\Omega_{\mathrm{SR}}}} K_1\left(\sqrt{\frac{4(\mathcal{A}+\mathcal{B})}{\Omega_{\mathrm{SR}}}}\right),\end{aligned} \tag{31}$$

where $\mathcal{A} = \frac{\gamma_{\mathrm{th}}}{\Omega_{\mathrm{RD}_1} a_1 \phi P_{\mathrm{S}}}$ and $\mathcal{B} = \frac{\gamma_{\mathrm{th}}}{\Omega_{\mathrm{RD}_2} \phi P_{\mathrm{S}} (1 - a_1(1+\gamma_{\mathrm{th}}))}$.

For the detailed derivations of $\mathcal{O}_{\mathrm{RD}}$, please refer to Appendix C.

Average packet delay of the buffer-aided relay system

In this section, the average packet delay of the system is considered. This delay includes the average packet delay at the source and the relay.

The average packet delay at the source is determined as

$$\mathcal{D}_{\mathrm{S}} = \frac{1+\mathcal{OP}}{1-\mathcal{OP}}. \tag{32}$$

while the average packet delay at the relay is expressed as

$$\mathcal{D}_{\mathrm{R}} = \frac{2}{1-\mathcal{OP}} \sum_{i=2}^{L+1} \pi_i (i-1). \tag{33}$$

Therefore, the average packet delay of the system is given by

$$\mathcal{D} = \mathcal{D}_{\mathrm{S}} + \mathcal{D}_{\mathrm{R}}. \tag{34}$$

Results and Discussion

In this section, detailed numerical results are provided to illustrate the impact of power allocation on the performance of SWIPT-NOMA system in terms of the OP and the EC. For comparison, we also provide the performance of the SWIPT-OMA system with the same parameters. Configurations and parameters of the system are explained as follows. D_1 is closer to the relay nodes than D_2. Hence, we need to allocate more power to D_2 than D_1 to ensure the user fairness. The optimal power allocation coefficient is derived in Theorem 3. The power allocation coefficient for D_1 is fixed at $a_1 = 0.3$ and that for D_2 is $1 - a_1$. The energy harvesting fraction $\alpha = 0.3$ and the energy conversion efficiency $\eta = 0.8$. The system data rate $r_1 = 1$ while $r_2 = r_0 = 0.5[b/s/Hz]$. The obtained numerical results show that the optimal power allocation can increase the system performance and the NOMA scheme significantly improves the spectrum utilization.

Fig. 4 illustrates the overall outage probability in terms of the average SNR in dB for two cases, i.e., with and without buffer-aided data at the relay node. As observed from Fig. 4, the overall outage probability of the system (including the outage events of both D_1 and D_2) in the case of optimal power allocation outperforms the case of fixed power allocation. From Fig 4, we can see that the benefit of the optimal power allocation in terms of the overall OP compared with the fixed power allocation is not significant. This is because we have choose the fixed power allocation $a_1 = 0.3$, which is the approximate of the optimal power allocation a_1^* (when $\alpha = 0.3$ and $r = 0.5$ returns $a_1^* = 0.2709$). In order to achieve the fairness of the overall system performance, the transmitter needs to allocate power according to the channel gains of $\mathrm{R} \rightarrow \mathrm{D}_1$ and $\mathrm{R} \rightarrow \mathrm{D}_2$. Furthermore, the approximation results calculated from (10) are very close to the exact results obtained from (9), especially at high SNR regime. Therefore, we can use (10) to calculate the OOP of the system easily. We can also see in Fig. 4 that the diversity order of the system with buffer aid is equal to 2. Meanwhile, for the case of without buffer-aided relaying, the diversity order of the system is equal to 1. Hence, employing data buffer at the relay leads to the reduction of OP, but it trades off with the packet delay. We can also see that the analytical results agree well with the simulation results.

Fig. 5 plots the overall OP and the OP of D_1 and D_2, respectively. The optimal power allocation coefficient as presented in Theorem 3 is used for both cases with and without buffer aided data at the relay node. We can see that the outage performance of D_1 is better than D_2. This is because the distance from the relay to D_2 is longer than that from the relay to D_1 [29] [6] The overall OP is calculated as the probability of the events that both D_1 and D_2 cannot decode their symbols successfully. The simulation and analytical results are in exellent match, validating the correctness of the closed-form expressions of (9), (12) and (13). From Fig. 5, we can observe that the joint outage events of D_1 and D_2 are less than each individual outage event of D_1 and D_2. This is suitable in practice where the probability that both D_1 and D_2 are in outage is always less than the probability that D_1 or D_2 is in outage.

The OP_{D_1} and OP_{D_2} are shown in Fig. 6 and Fig. 7, respectively. The power allocation coefficient is fixed at $a_1 = 0.3$ when investigating the outage performance of both OP_{D_1} and OP_{D_2}. Moreover, we also conduct the optimal power allocation for the relay as described in the Theorem 3. Again, we can see that the analytical results are in excellent agreement with the simulation results. From these figures we can see that the NOMA system with the optimal power allocation has better outage performance than the OMA system. In the case of fixed power allocation, the outage performance of D_1 is better than the OMA system, but outage performance of D_2 is worse than the OMA system. However, the NOMA system provides better spectral efficiency because two users are served simultaneously. Different from Fig 4, the gap of the curves plotted in Fig 6 and Fig 7 is more significant for the two cases with fixed and optimal power allocation. The reason is that the probability of the event that both D_1 and D_2 are in outage is less than the probability of each event that D_1 or D_2 is in outage.

Fig. 8 depicts the effect of the power allocation coefficient on the OP. It should be noted that we only define the coefficient for D_2 while the coefficient for D_1 is

---

[6] The signal power of far-field RF transmission is reduced according to the mutual distance between receiver and transmitter, specifically, $20dB$ per decade of the distance.

derived from the condition $a_2 = 1 - a_1$. As shown in Fig. 8, different data rates r_2 exhibit different minimum values of the OP. In this figure we can see that when the rate transmission r_2 is reduced, the power allocation coefficient for D_2 decreases to get better system performance for the fairness of the outage performance of D_1 and D_2.

The system ergodic capacity is shown in Fig. 9. According to the NOMA theory, the ergodic capacity of the system is the summation of the ergodic capacity of all users. Let β and $(1-\beta)$ [Hz] denote the bandwidth assigned for D_1 and the remaining bandwidth assigned for D_2, where $(0 \le \beta \le 1)$. Using [30, eq. (7.4)], the sum capacity of the OMA system is given by

$$\begin{aligned} C_{OMA} = & \frac{1-\alpha}{2}\beta \log_2\left(1+\min\left\{\frac{P_S|h_1|^2}{\beta}, \frac{P_R|g_1|^2}{\beta}\right\}\right) \\ & + \frac{(1-\alpha)(1-\beta)}{2}\log_2\left(1+\min\left\{\frac{P_S|h_1|^2}{1-\beta}, \frac{P_R|g_2|^2}{1-\beta}\right\}\right). \end{aligned} \quad (35)$$

From Fig. 9, we can see that the ergodic capacity of the NOMA system is better than the OMA system. Additionally, the ergodic capacity of D_1 in our proposed system is better than that in the OMA system. However, the ergodic capacity of D_2 is not higher than OMA system due to the poor channel condition from the relay to the D_2. Therefore, the advantage of the NOMA system is to improve the capacity significantly. We also see that the analytical results are very close to the simulation results because we use an approximation of the CDF of X_2 as given in (56).

Conclusion

In this paper, we proposed a NOMA cooperative relaying network with and without data buffer-aided relay. In addition, the relay node harvests the energy from the source using the time-switching mechanism. We focus on deriving the OP and ergodic capacity of the system over Rayleigh fading channels. Moreover, we proposed a power allocation scheme at the relay node which aims to reduce the feedback cost. Numerical results of the OP and capacity showed that the proposed NOMA downlink relaying system significantly outperformed the OMA system. The data buffer aid employed at the relay helps improve the performance of the system. However, the proposed system trades off with the permissible packet delay. All closed-form expressions derived in this paper were verified by the Monte-Carlo simulations.

The impact of fixed and optimal power allocation on the performance of EH-NOMA downlink relaying network was also investigated. In this model, all nodes are equipped with a single antenna. However, it can be developed for multiple antenna systems.

Our proposed relaying network can achieve two goals: (i) the energy efficiency is improved by the harvested energy from the ambient RF environment. This idea can be applied to sensor nodes in wireless body area networks for healthcare and other medical applications, (ii) the spectrum utilizing efficiency is superior to that of the OMA system. It is a promising application which can enhance the performance of the 5G networks and the wireless sensor and healthcare networks.

Appendix A

The goal of this appendix is to provide the overall OP of the SWIPT-NOMA system over Rayleigh fading channels.

The overall OP of the system can be expressed as

$$\mathrm{OOP} = \underbrace{\Pr\left(\gamma_{\mathrm{R}} \leq \gamma_{\mathrm{th}}\right)}_{\mathrm{OP}_1} + \underbrace{\Pr\left(\gamma_{\mathrm{R}} > \gamma_{\mathrm{th}},\, \max\left(\gamma_{\mathrm{D}_1}^{x_1},\, \gamma_{\mathrm{D}_2}^{x_2},\, \gamma_{\mathrm{D}_1}^{x_2\to x_1}\right) \leq \gamma_{\mathrm{th}}\right)}_{\mathrm{OP}_2}. \quad (36)$$

From (2), we obtain the closed-form expression of the first term of (36) as

$$\mathrm{OP}_1 = \Pr\left(|h_1|^2 \leq \frac{\gamma_{\mathrm{th}}}{P_{\mathrm{S}}}\right) = 1 - \exp\left(-\frac{\gamma_{\mathrm{th}}}{\Omega_1 P_{\mathrm{S}}}\right). \quad (37)$$

To obtain the closed-form expression of the second term of (36), we rewrite the second term of (36) as follows

$$\mathrm{OP}_2 = \Pr\left(\gamma_{\mathrm{R}} > \gamma_{\mathrm{th}},\, \gamma_{\mathrm{D}_1}^{x_1} \leq \gamma_{\mathrm{th}}, \gamma_{\mathrm{D}_1}^{x_2\to x_1} < \gamma_{\mathrm{th}}\,, \gamma_{\mathrm{D}_2}^{x_2} < \gamma_{\mathrm{th}}\right). \quad (38)$$

From (38) and the condition in (11), i.e. $\gamma_{\mathrm{D}_1}^{x_2\to x_1} > \gamma_{\mathrm{D}_2}^{x_2}$, we have

$$\mathrm{OP}_2 = \Pr\left(\gamma_{\mathrm{R}} > \gamma_{\mathrm{th}},\, \gamma_{\mathrm{D}_1}^{x_1} \leq \gamma_{\mathrm{th}}, \gamma_{\mathrm{D}_1}^{x_2\to x_1} < \gamma_{\mathrm{th}}\right). \quad (39)$$

By substituting (2), (7), and (8) into (39) and denoting $|h_1|^2 = X$, $|g_1|^2 = Y$ and $|g_2|^2 = Z$, we obtain:

$$\mathrm{OP}_2 = \Pr\left(X > \frac{\gamma_{\mathrm{th}}}{P_S}, XY \leq \frac{\gamma_{\mathrm{th}}}{a_1 \phi P_{\mathrm{S}}}, XY < \frac{\gamma_{\mathrm{th}}}{\phi P_{\mathrm{S}}(a_2 - a_1\gamma_{\mathrm{th}})}\right). \tag{40}$$

As can be seen from (40), the outage always occurs if $a_1 \geq \frac{1}{1+\gamma_{\mathrm{th}}}$. Thus, allocating more power to the D_2 is required so that $1 - a_1(1+\gamma_{\mathrm{th}}) > 0$ always holds. The condition $a_1 < \frac{1}{1+\gamma_{\mathrm{th}}}$ is used throughout this paper. For simplicity, we can rewrite (40) as

$$\mathrm{OP}_2 = \Pr\left(X > \frac{\gamma_{\mathrm{th}}}{P_{\mathrm{S}}}, XY \leq \Psi_{\min}\right), \tag{41}$$

where $\Psi_{\min} = \min\left\{\frac{\gamma_{\mathrm{th}}}{a_1\phi P_{\mathrm{S}}}, \frac{\gamma_{\mathrm{th}}}{\phi P_{\mathrm{S}}(1-a_1(1+\gamma_{\mathrm{th}}))}\right\}$.

Based on the conditional probability [31] and the assumption that the channel gains have exponential distributions, we have

$$\mathrm{OP}_2 = \int_{\frac{\gamma_{\mathrm{th}}}{P_{\mathrm{S}}}}^{\infty} F_Y\left(\frac{\Psi_{\min}}{x}\right) f_X(x)dx = \int_{\frac{\gamma_{\mathrm{th}}}{P_{\mathrm{S}}}}^{\infty} \left[1 - \exp\left(\frac{\Psi_{\min}}{\Omega_2 x}\right)\right] f_X(x)dx, \tag{42}$$

where $F_Y(y) = 1 - \exp\left(-\frac{y}{\Omega_2}\right)$ and $f_X(x) = \frac{1}{\Omega_1}\exp\left(-\frac{x}{\Omega_1}\right)$ are the CDF of X and the PDF of Y, respectively.

Substituting PDF of X into (42) yields

$$\mathrm{OP}_2 = \exp\left(-\frac{\gamma_{\mathrm{th}}}{\Omega_1 P_{\mathrm{S}}}\right) - \frac{1}{\Omega_1}\int_{\frac{\gamma_{\mathrm{th}}}{P_{\mathrm{S}}}}^{\infty} \exp\left(-\frac{\Psi_{\min}}{\Omega_2 x} - \frac{x}{\Omega_1}\right) dx. \tag{43}$$

By using the Taylor series expansions of the exponential function and after some manipulations on (43) using [27, 3.351.4], we obtain the second term of (36) as given in (44) below.

$$\mathrm{OP}_2 = \exp\left(-\frac{\gamma_{\mathrm{th}}}{\Omega_1 P_{\mathrm{S}}}\right) - \frac{1}{\Omega_1}\sum_{k=0}^{\infty}\frac{(-1)^k}{k!}\left(\frac{\Psi_{\min}}{\Omega_2}\right)^k$$
$$\left[\frac{(-1)^k}{(k-1)!}\left(\frac{1}{\Omega_1}\right)^{k-1}\mathrm{Ei}\left(\frac{-\gamma_{\mathrm{th}}}{\Omega_1 P_{\mathrm{S}}}\right) + \frac{\exp\left(\frac{-\gamma_{\mathrm{th}}}{\Omega_1 P_{\mathrm{S}}}\right)}{\left(\frac{\gamma_{\mathrm{th}}}{P_{\mathrm{S}}}\right)^{k-1}}\sum_{j=0}^{k-2}\frac{(-1)^j\left(\frac{\gamma_{\mathrm{th}}}{\Omega_x P_{\mathrm{S}}}\right)^j}{\prod_{\ell=0}^{j}(k-1-\ell)}\right]. \tag{44}$$

We obtain the OP expression of the system by combining (37) and (44). When the transmission power is high, we have $\gamma_{\rm th} \ll P_{\rm S}$. Then, (43) can be approximated as

$$\mathrm{OP}_2 = 1 - \frac{1}{\Omega_1}\int_0^\infty \exp\left(-\frac{\Psi_{\min}}{\Omega_2 x} - \frac{x}{\Omega_1}\right) dx. \tag{45}$$

From (45), by using [27, 3.324.1], i.e. $\int_0^\infty e^{\frac{-\beta}{4x} - \gamma x} = \sqrt{\frac{\beta}{\gamma}} K_1\left(\sqrt{\beta\gamma}\right)$, and after some mathematical manipulations, we have the approximation of (10) at high SNR regime. The proof of Theorem 1 is completed.

Appendix B

Due to the imperfect detection at the relay node, it may forward wrong decoded signals to D_1 and D_2 and cannot apply SIC technique on symbol x_2 at the D_1. Hence similar to [32], for any modulation scheme, the dual-hop of the links $\mathrm{S} \to \mathrm{R} \to \mathrm{D}_1$ or $\mathrm{S} \to \mathrm{R} \to \mathrm{D}_2$ can be modeled as an equivalent one-hop channel whose output SINR $\mathcal{X}_i$, $i \in \{1,2\}$ at high SNR regime can be tightly approximated.

Let denote $\mathcal{X}_1$ and $\mathcal{X}_2$ the SINRs obtained at D_1 and D_2, respectively [5].

$$\mathcal{X}_1 = \min\left(\gamma_{\rm R}, \gamma_{\rm D_1}^{x_1}, \gamma_{\rm D_1}^{x_2 \to x_1}\right), \tag{46}$$

$$\mathcal{X}_2 = \min\left(\gamma_{\rm R}, \gamma_{\rm D_2}^{x_2}\right). \tag{47}$$

To find the OP of D_1, from (46), we have the OP expression of D_1 as

$$\begin{aligned}\mathrm{OP}_{\rm D_1} &= 1 - \Pr\left(\gamma_{\rm R} > \xi_1, \gamma_{D_1}^{x_1} > \xi_1, \gamma_{D_1}^{x_2 \to x_1} > \xi_1\right) \\ &= 1 - \Pr\left(X > \frac{\xi_1}{P_{\rm S}}, XY \geq \mathcal{Q}_{\max}\right),\end{aligned} \tag{48}$$

where $\mathcal{Q}_{\max} = \max\left\{\frac{\xi_1}{a_1\phi P_{\rm S}}, \frac{\xi_1}{\phi P_{\rm S}(1 - a_1(1+\xi_1))}\right\}$.

By using the conditional probability [31], we can rewrite (48) as

$$\mathrm{OP}_{\rm D_1} = 1 - \int_{\frac{\xi_1}{P_{\rm S}}}^\infty \left[1 - F_Y\left(\frac{\mathcal{Q}_{\max}}{x}\right)\right] f_X(x) dx. \tag{49}$$

Since the CDF and PDF of X and Y are exponential distribution functions, we have

$$\mathrm{OP}_{\mathrm{D}_1} = 1 - \frac{1}{\Omega_x}\int_{\frac{\xi_1}{P_\mathrm{S}}}^{\infty} \exp\left(-\frac{\mathcal{Q}_{\max}}{\Omega_2 x}\right)\exp\left(-\frac{x}{\Omega_1}\right)dx. \tag{50}$$

By using the Taylor series expansions of the exponential function and after some manipulations on (50) using [27, 3.351.4], we have the expression of the OP of D_1 as presented in (12).

Next, we calculate the OP expression at D_2. With the given SINR at the D_2 and the notation $\mathcal{X}_2 = \min(\gamma_\mathrm{R}, \gamma_{D_2}^{x_2})$, we have

$$\mathrm{OP}_{\mathrm{D}_2} = \Pr\left(\min(\gamma_\mathrm{R}, \gamma_{\mathrm{D}_2}^{x_2}) \le \xi_2\right) = 1 - \Pr\left(\gamma_\mathrm{R} > \xi_2, \gamma_{\mathrm{D}_2}^{x_2} > \xi_2\right). \tag{51}$$

Substituting (2) and (6) into (51) yields

$$\begin{aligned}\mathrm{OP}_{\mathrm{D}_2} &= 1 - \Pr\left(\frac{P_\mathrm{S}|h_1|^2}{N_0} > \xi_2, \frac{a_2 P_\mathrm{R}|g_2|^2}{a_1 P_\mathrm{R}|g_2|^2 + N_0} > \xi_2\right) \\ &= 1 - \Pr\left(X > \frac{\xi_2}{P_\mathrm{S}}, XZ > \frac{\xi_2}{\phi P_\mathrm{S}\left(a_2 - a_1\xi_2\right)}\right)\end{aligned} \tag{52}$$

Then, by applying similar calculations in Appendix A we can obtain the OP of D_2 as

$$\begin{aligned}\mathrm{OP}_{\mathrm{D}_2} &= 1 - \int_{\frac{\xi_2}{P_\mathrm{S}}}^{\infty}\left[1 - F_Z\left(\frac{\xi_2}{x\phi P_\mathrm{S}\left(a_2 - a_1\xi_2\right)}\right)\right] f_X(x)\,dx \\ &= 1 - \frac{1}{\Omega_1}\int_{\frac{\xi_2}{P_\mathrm{S}}}^{\infty}\exp\left(-\frac{b}{x\Omega_2}\right)\exp\left(-\frac{x}{\Omega_2}\right)dx.\end{aligned} \tag{53}$$

By using the Taylor series expansions of the exponential function $\exp\left(-\frac{b}{x\Omega_2}\right) = \sum_{t=0}^{\infty}\frac{(-1)^t}{t!}\left(\frac{b}{x\Omega_2}\right)^t$, after some manipulations of (53) using [27, 3.351.4], we obtain the closed-form expression of the OP of D_2 as given in (13). The proof of Theorem 2 is completed.

Appendix C

From (6) and (8), the expression of $\mathcal{O}_{\mathrm{RD}}$ is expressed as

$$\begin{aligned}
\mathcal{O}_{\mathrm{RD}} &= \Pr\left(\max\left(\gamma_{\mathrm{D}_1}^{x_1}, \gamma_{\mathrm{D}_2}^{x_2}\right) < \gamma_{\mathrm{th}}\right) \\
&= \Pr\left(\frac{a_1 P_{\mathrm{R}} |g_1|^2}{N_0} < \gamma_{\mathrm{th}}, \frac{(1-a_1) P_{\mathrm{R}} |g_2|^2}{a_1 P_{\mathrm{R}} |g_2|^2 + 1} < \gamma_{\mathrm{th}}\right) \\
&= \Pr\left(XY < \frac{\gamma_{\mathrm{th}}}{a_1 \phi P_{\mathrm{S}}}, XZ < \frac{\gamma_{\mathrm{th}}}{\phi P_{\mathrm{S}}(1 - a_1(1+\gamma_{\mathrm{th}}))}\right).
\end{aligned} \tag{54}$$

Based on the definition of the conditional probability, we have

$$\begin{aligned}
\mathcal{O}_{\mathrm{RD}} &= \int_0^\infty \Pr\left(Y < \frac{\mathcal{A}}{x}, Z < \frac{\mathcal{B}}{x}\right) f_X(x) dx \\
&= \int_0^\infty \int_0^{\frac{\mathcal{B}}{x}} \Pr\left(Y < \frac{\mathcal{A}}{x}\right) f_Z(z) f_X(x) dx dz \\
&= \int_0^\infty \left[1 - e^{\left(-\frac{\mathcal{A}}{x}\right)} - e^{\left(-\frac{\mathcal{B}}{x}\right)} + e^{\left(-\frac{\mathcal{A}}{x} - \frac{\mathcal{B}}{x}\right)}\right] f_X(x) dx,
\end{aligned} \tag{55}$$

where $\mathcal{A} = \frac{\gamma_{\mathrm{th}}}{a_1 \phi P_{\mathrm{S}}}$, $\mathcal{B} = \frac{\gamma_{\mathrm{th}}}{\phi P_{\mathrm{S}}(1 - a_1(1+\gamma_{\mathrm{th}}))}$. After some manipulations, we get (31), completing the proof of Theorem 4.

Appendix D

This appendix aims to provide the CDF of the instantaneous SNR of the information symbol x_1. The instantaneous end-to-end SNR of symbol x_1 is $X_1 = \min\left(\gamma^{\mathrm{R}}, \gamma_{x_1}^{\mathrm{D}_1}\right)$. Thus, the CDF of X_1 is given by

$$\begin{aligned}
F_{X_1}(\xi_1) &= \Pr\left(\min\left(\gamma^{\mathrm{R}}, \gamma_{x_1}^{\mathrm{D}_1}\right) \le \xi_1\right) \\
&= 1 - \Pr\left(P_S |h_1|^2 > \xi_1,\, a_1 \phi P_S |h_1|^2 |g_1|^2 > \xi_1\right) \\
&= 1 - \frac{1}{\Omega_1} \int_{\frac{\xi_1}{P_S}}^{\infty} \exp\left(-\frac{\xi_1}{\Omega_2 a_1 \phi P_S x} - \frac{x}{\Omega_1}\right) dx \\
&\approx 1 - \sqrt{\frac{4\xi_1}{\Omega_1 \Omega_2 a_1 \phi P_{\mathrm{S}}}} K_1\left(\sqrt{\frac{4\xi_1}{\Omega_1 \Omega_2 a_1 \phi P_{\mathrm{S}}}}\right).
\end{aligned} \tag{56}$$

Acknowledgements

Not applicable.

Funding

There is no funding support for this paper.

Abbreviations

5G	Fifth Generation
AWGN	Additive White Gaussian Noise
CDF	Cumulative Distribution Function
CR-NOMA	Cognitive Radio Non-Orthogonal Multiple Access
CSI	Channel State Information
DF	Decode-and-Forward
EH	Energy Harvesting
F-NOMA	Fixed-power-allocation Non-Orthogonal Multiple Access
IoT	Internet of Things
NOMA	Non-Orthogonal Multiple Access
OMA	Orthogonal Multiple Access
OOP	Overall Outage Probability
OP	Outage Probability
PDF	Probability Density Function
PS	Power Splitting
RF	Radio Frequency
RV	Random Variable
SINR	Signal-to-Interference-and-Noise Ratio
SNR	Signal-to-Noise Ratio
SWIPT	Simultaneous Wireless Information and Power Transfer
TDD	Time Division Duplex
TS	Time Switching

Availability of data and materials

All necessary data and materials have been presented in this paper. There are no extra data and materials to share.

Ethics approval and consent to participate

Not applicable.

Competing interests

The authors declare that they have no competing interests.

Consent for publication

Not applicable.

Authors' contributions

N.T.T. created the main ideas and formulates the problem; T.M.H. executed performance evaluation by rigorous analysis and wrote the original draft; B.C.N. wrote simulation programs; P.T.T. worked as an advisor of the project to discuss and advise the main ideas, provided recommendations on performance evaluation, and edited the final manuscript.

Authors' information

N. N. Thang received the B.S. degree in Le Quy Don Technical University, in 1991, the M.S. degree and the Ph.D. degree in Le Quy Don Technical University, Hanoi, Vietnam, in 1997 and 2017, respectively. His major interests are antenna, wireless communication and cooperative communication. E-mail: nguyennhuthang@tcu.edu.vn.

T. M. Hoang was born in November 07, 1977. He received the B.S. degree in Communication Command at Telecommunications University, Ministry of Defense, Vietnam, in 2002, and the B.Eng. degree in Electrical Engineering from Le Quy Don Technical University, Ha Noi, Vietnam, in 2006. He obtained the M.Eng. degree in Electronics Engineering from Posts and Telecommunications, Institute of Technology, (VNPT), Vietnam, in 2013. He is currently pursuing the Ph.D degree at Le Quy Don Technical University, Hanoi, Vietnam. His research interests include energy harvesting, Non-Orthogonal Multiple Access, and signal processing for wireless cooperative communications. E-mail: tranmanhhoang@tcu.edu.vn.

B. C. Nguyen was born in Nghean, Vietnam. He received the B.S. in 2006 in Telecommunication University and M.S. in 2011 in Posts and Telecommunications, Institute of Technology, (VNPT), Vietnam. He is currently pursuing the Ph.D degree at Le Quy Don Technical University, Hanoi, Vietnam. His research interests include energy harvesting, full-duplex, and cooperative communication. E-mail: bacao.sqtt@gmail.com.

P. T. Tran was born at Ho Chi Minh City, Vietnam, in 1979. He received B.Eng. and M.Eng degrees in electrical engineering from Ho Chi Minh University of Technology, Ho Chi Minh City, Vietnam in 2002 and 2005, respectively. In 2007, he became a Vietnam Education Foundation Fellow at Purdue University, U.S.A., where he received his M.S. degree in mathematics and Ph.D. degree in electrical and computer engineering in 2013. In 2013, he joined the Faculty of Electrical and Electronics Engineering of Ton Duc Thang University, Vietnam and served as the Vice Dean of Faculty since October 2014. He is currently an IEEE Senior Member. His major interests are in the area of wireless communications and network information theory. Email: tranthanhphuong@tdtu.edu.vn.

Author details

[1]Nha Trang Telecommunications University, Nha Trang, Vietnam. [2]Wireless Communications Research Group, Faculty of Electrical and Electronics Engineering, Ton Duc Thang University., Ho Chi Minh City, Vietnam.

References

1. Wang, Y., Ren, B., Sun, S., Kang, S., Yue, X.: Analysis of Non-Orthogonal Multiple Access for 5G. China Commun. **13**(Supplement No.2), 52–66 (2016)
2. Dai, L., Wang, B., Yuan, Y., Han, S., I, C.-L., Wang, Z.: Non-Orthogonal Multiple Access for 5G: Solutions, Challenges, Opportunities, and Future Research Trends **53**(9), 74–81 (2015)
3. Yang, Z., Ding, Z., Fan, P., Al-Dhahir, N.: The Impact of Power Allocation on Cooperative Non-orthogonal Multiple Access Networks with SWIPT **16**(7), 4332–4343 (2017)
4. Luo, S., Teh, K.C.: Adaptive transmission for cooperative NOMA system with Buffer-Aided Relaying **21**(4), 937–940 (2017)
5. Kader, M.F., Shahab, M.B., Shin, S.-Y.: Exploiting Non-orthogonal Multiple Access in Cooperative Relay Sharing **21**(5), 1159–1162 (2017)
6. Du, C., Chen, X., Lei, L.: Energy-Efficient Optimisation for Secrecy Wireless Information and Power Transfer in Massive MIMO Relaying Systems. IET Commun. **11**(1), 10–16 (2017)
7. Chen, Y.: Energy-Harvesting AF Relaying in the Presence of Interference and Nakagami-Fading **15**(2), 1008–1017 (2016)
8. Boshkovska, E., Ng, D.W.K., Zlatanov, N., Schober, R.: Practical non-linear energy harvesting model and resource allocation for SWIPT systems **19**(12), 2082–2085 (2015)
9. Ding, Z., Perlaza, S.M., Esnaola, I., Poor, H.V.: Power allocation strategies in energy harvesting wireless cooperative networks **13**(2), 846–860 (2014)
10. Varshney, L.R.: Transporting information and energy simultaneously, pp. 1612–1616 (2008). IEEE
11. Ashraf, M., Shahid, A., Jang, J.W., Lee, K.-G.: Energy Harvesting Non-Orthogonal Multiple Access System With Multi-Antenna Relay and Base Station. IEEE Access **5**, 17660–17670 (2017)
12. Sun, R., Wang, Y., Wang, X., Zhang, Y.: Transceiver design for cooperative non-orthogonal multiple access systems with wireless energy transfer. IET Commun. **10**(15), 1947–1955 (2016)
13. Han, W., Ge, J., Men, J.: Performance Analysis for NOMA Energy Harvesting Relaying Networks with Transmit Antenna Selection and Maximal-Ratio Combining over Nakagami-m Fading. IET Commun. **10**(18), 2687–2693 (2016)
14. Liu, Y., Ding, Z., Elkashlan, M., Poor, H.V.: Cooperative non-orthogonal multiple access with simultaneous wireless information and power transfer **34**(4), 938–953 (2016)
15. Bapatla, D., Prakriya, S.: Performance of a cooperative network with an energy buffer-aided relay **3**(3), 774–788 (2019)
16. Nomikos, N., Charalambous, T., Vouyioukas, D., Karagiannidis, G.K., Wichman, R.: Hybrid NOMA/OMA with buffer-aided relay selection in cooperative networks **13**(3), 524–537 (2019)
17. Manoj, B., Mallik, R.K., Bhatnagar, M.R.: Performance analysis of buffer-aided priority-based max-link relay selection in DF cooperative networks **66**(7), 2826–2839 (2018)
18. Xu, P., Quan, J., Yang, Z., Chen, G., Ding, Z.: Performance Analysis of Buffer-Aided Hybrid NOMA/OMA in Cooperative Uplink System. IEEE Access **7**, 168759–168773 (2019)

19. Zhang, Q., Liang, Z., Li, Q., Qin, J.: Buffer-aided non-orthogonal multiple access relaying systems in rayleigh fading channels **65**(1), 95–106 (2017)
20. Luo, S., Yang, G., Teh, K.C.: Throughput of wireless-powered relaying systems with buffer-aided hybrid relay **15**(7), 4790–4801 (2016)
21. Ju, H., Zhang, R.: Throughput Maximization in Wireless Powered Communication Networks **13**(1), 418–428 (2014)
22. Gu, Y., Aïssa, S.: RF-based energy harvesting in decode-and-forward relaying systems: Ergodic and outage capacities **14**(11), 6425–6434 (2015)
23. Nasir, A.A., Zhou, X., Durrani, S., Kennedy, R.A.: Relaying protocols for wireless energy harvesting and information processing **12**(7), 3622–3636 (2013)
24. Abdelhady, A.M., Amin, O., Shihada, B., Alouini, M.-S.: Spectral efficiency and energy harvesting in multi-cell slipt systems (2020)
25. Tran, H.M., Nguyen, C.B., Tran, P.T., Le, D.T.: Outage analysis of rf energy harvesting cooperative communication systems over nakagami-m fading channels with integer and non-integer m (2020)
26. Pedersen, K.I., Kolding, T.E., Seskar, I., Holtzman, J.M.: Practical implementation of successive interference cancellation in DS/CDMA systems. In: Universal Personal Communications, 1996. Record., 1996 5th IEEE International Conference On, vol. 1, pp. 321–325 (1996). IEEE
27. Zwillinger, D.: Table of Integrals, Series, and Products. Elsevier, ??? (2014)
28. Boyd, S., Vandenberghe, L.: Convex Optimization. Cambridge University Press, ??? (2004)
29. Lu, X., Wang, P., Niyato, D., Kim, D.I., Han, Z.: Wireless networks with RF energy harvesting: A contemporary survey. IEEE Commun. Tutorials **17**(2), 757–789 (2015)
30. Benjebbour, A., Saito, K., Li, A., Kishiyama, Y., Nakamura, T.: Non-Orthogonal Multiple Access (NOMA): Concept and Design. Signal Processing for 5G: Algorithms and Implementations, 143–168 (2016)
31. Papoulis, A., Pillai, S.U.: Probability, Random Variables, and Stochastic Processes. Tata McGraw-Hill Education, ??? (2002)
32. Wang, T., Cano, A., Giannakis, G.B., Laneman, J.N.: High-performance cooperative demodulation with decode-and-forward relays **55**(7), 1427–1438 (2007)

[width=2.5in]Fig1SM.pdf

Figure 1 Wirelessly powered NOMA downlink relaying network

[width=2.5in]markov1.pdf

Figure 2 The diagram of the Markov chain of buffer states at the relay node.

[width=2.5in]Fig7.eps

Figure 3 The average packet delay versus SNR according to theorycal analysis.

[width=2.5in]Fig1.eps

Figure 4 Overall outage probability versus average SNRs for optimal and fixed power allocation.

[width=2.5in]Fig4.eps

Figure 5 Outage probability versus the SNR with optimal power allocation for the cases of with buffer and without buffer aided relaying.

[width=2.5in]Fig2.eps

Figure 6 Outage probability of D_1 versus the transmission power of the source for optimal and fixed power allocation.

[width=2.5in]Fig3.eps

Figure 7 Outage probability of D_2 versus its SNR for the cases of optimal power allocation and fixed power allocation.

[width=2.5in]Fig5.eps

Figure 8 The effect of power allocation coefficient on the OP for different data rates, EbNo = 10dB.

[width=2.5in]Fig6.eps

Figure 9 Average capacity of the system versus its SNR.

Figures

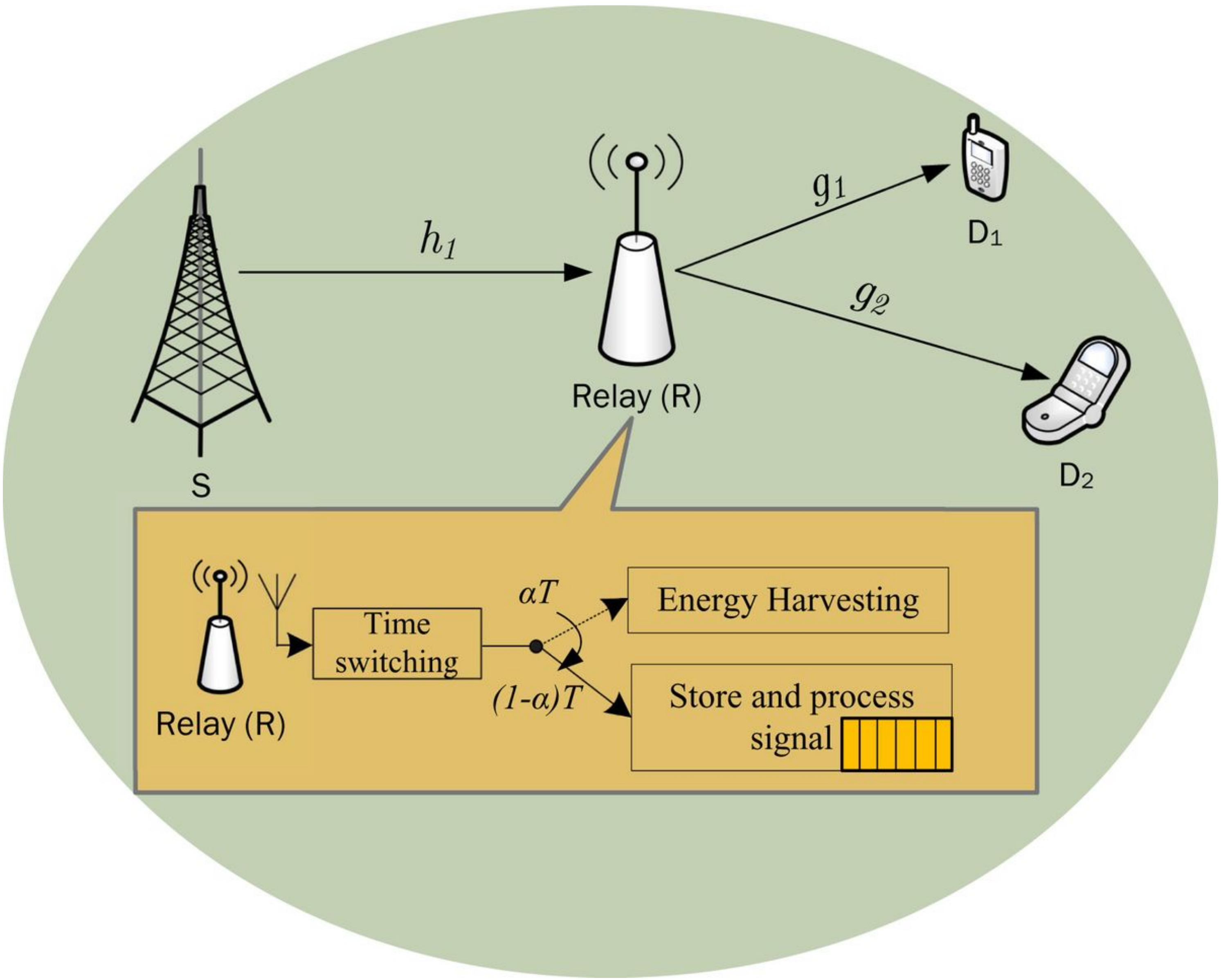

Figure 1

Wirelessly powered NOMA downlink relaying network

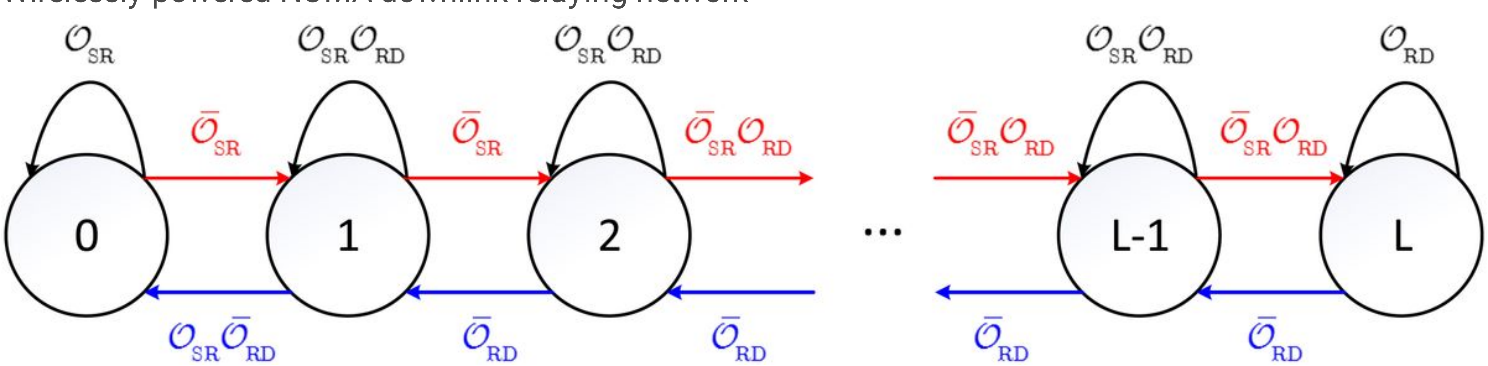

Figure 2

The diagram of the Markov chain of buffer states at the relay node.

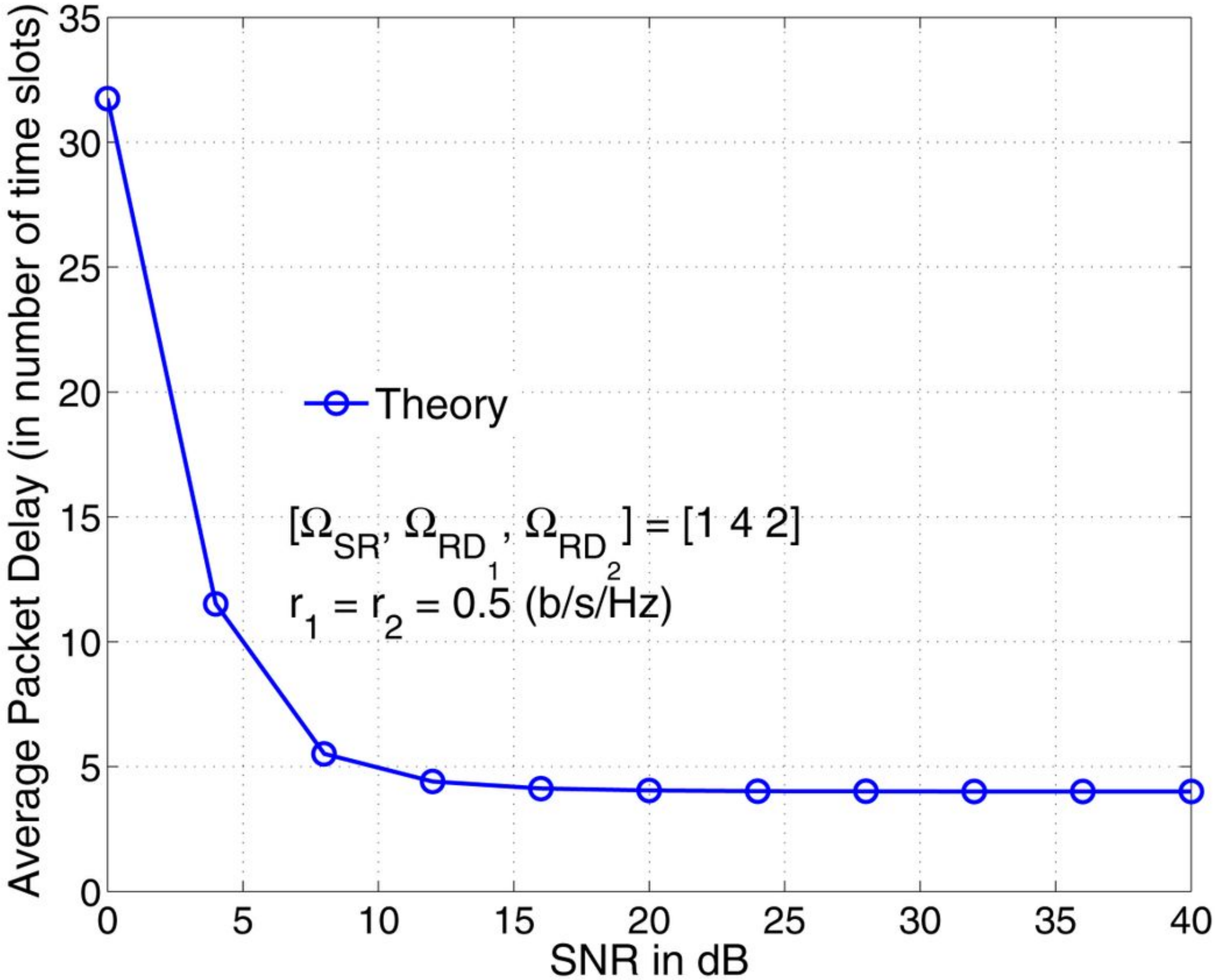

Figure 3

The average packet delay versus SNR according to theorycal analysis.

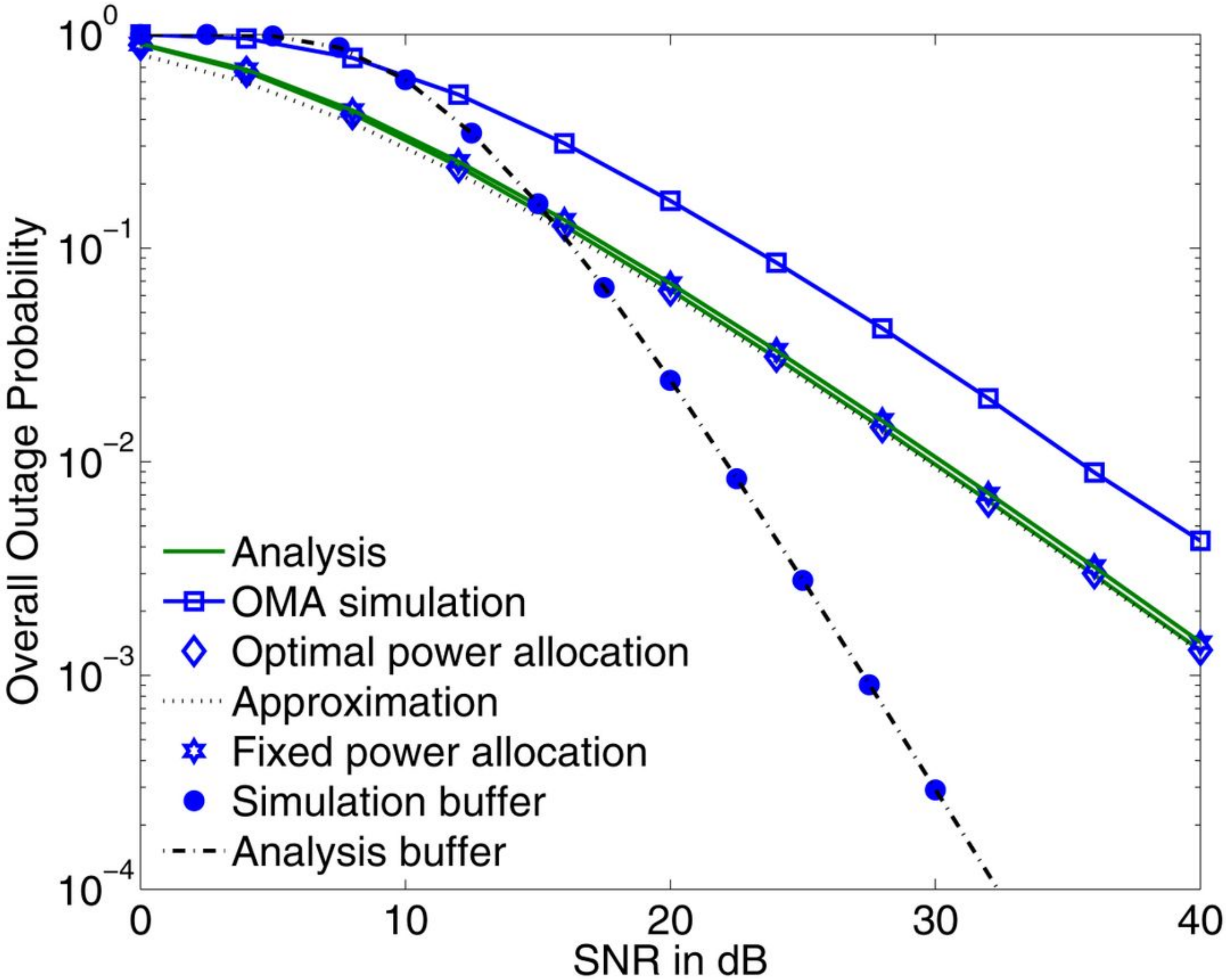

Figure 4

Overall outage probability versus average SNRs for optimal and fixed power allocation.

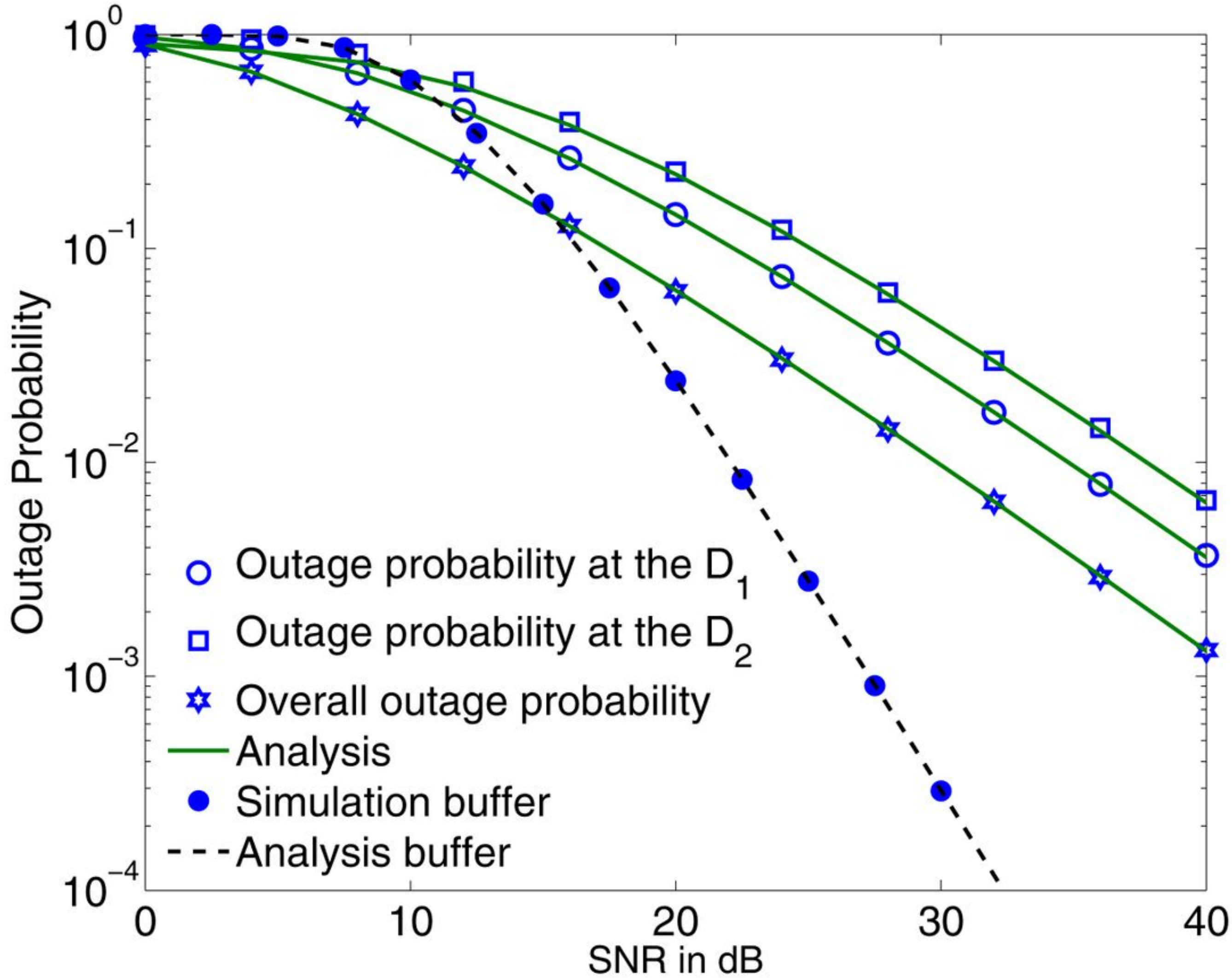

Figure 5

Outage probability versus the SNR with optimal power allocation for the cases of with buffer and without buffer aided relaying.

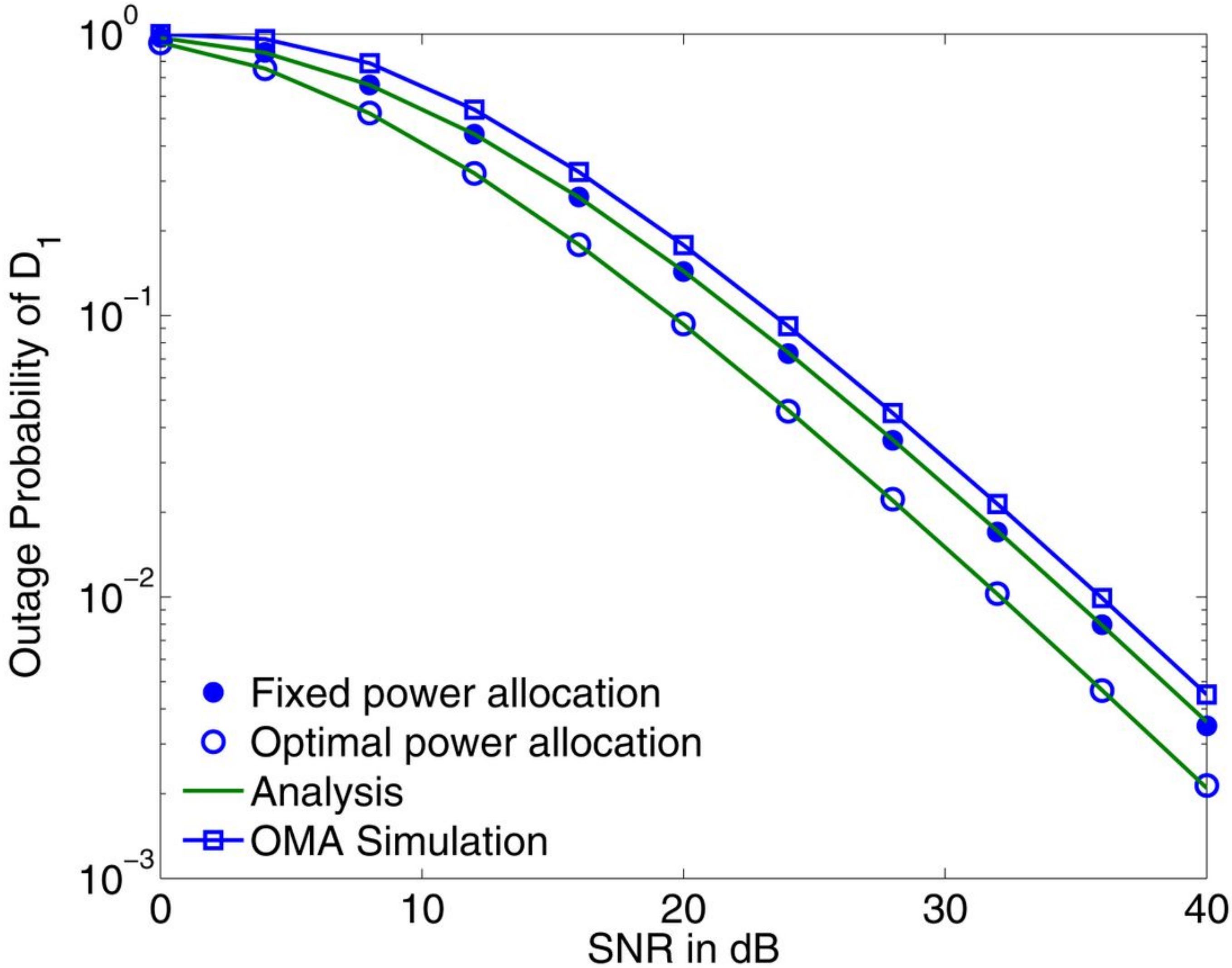

Figure 6

Outage probability of D1 versus the transmission power of the source for optimal and fixed power allocation.

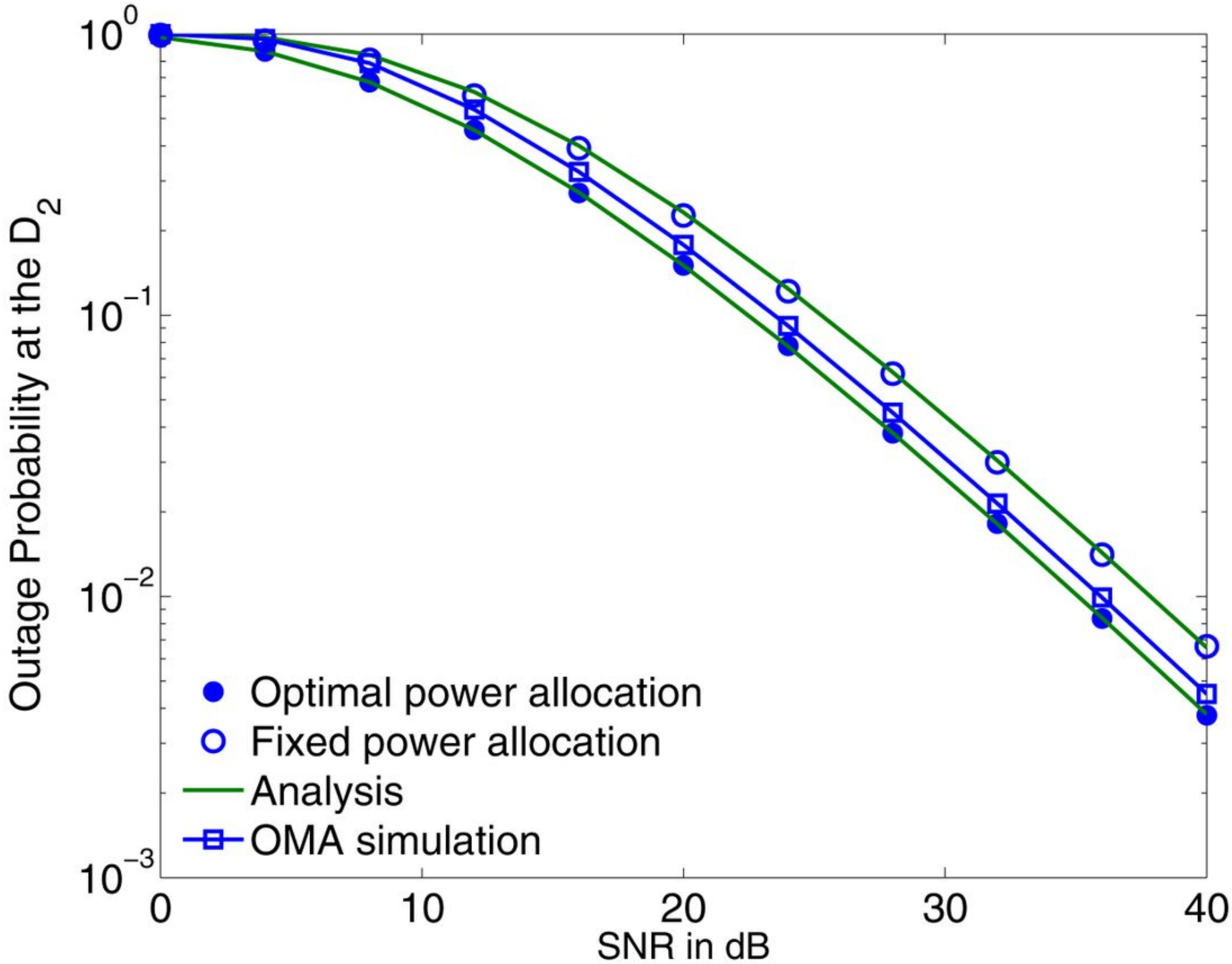

Figure 7

Outage probability of D2 versus its SNR for the cases of optimal power allocation and xed power allocation.

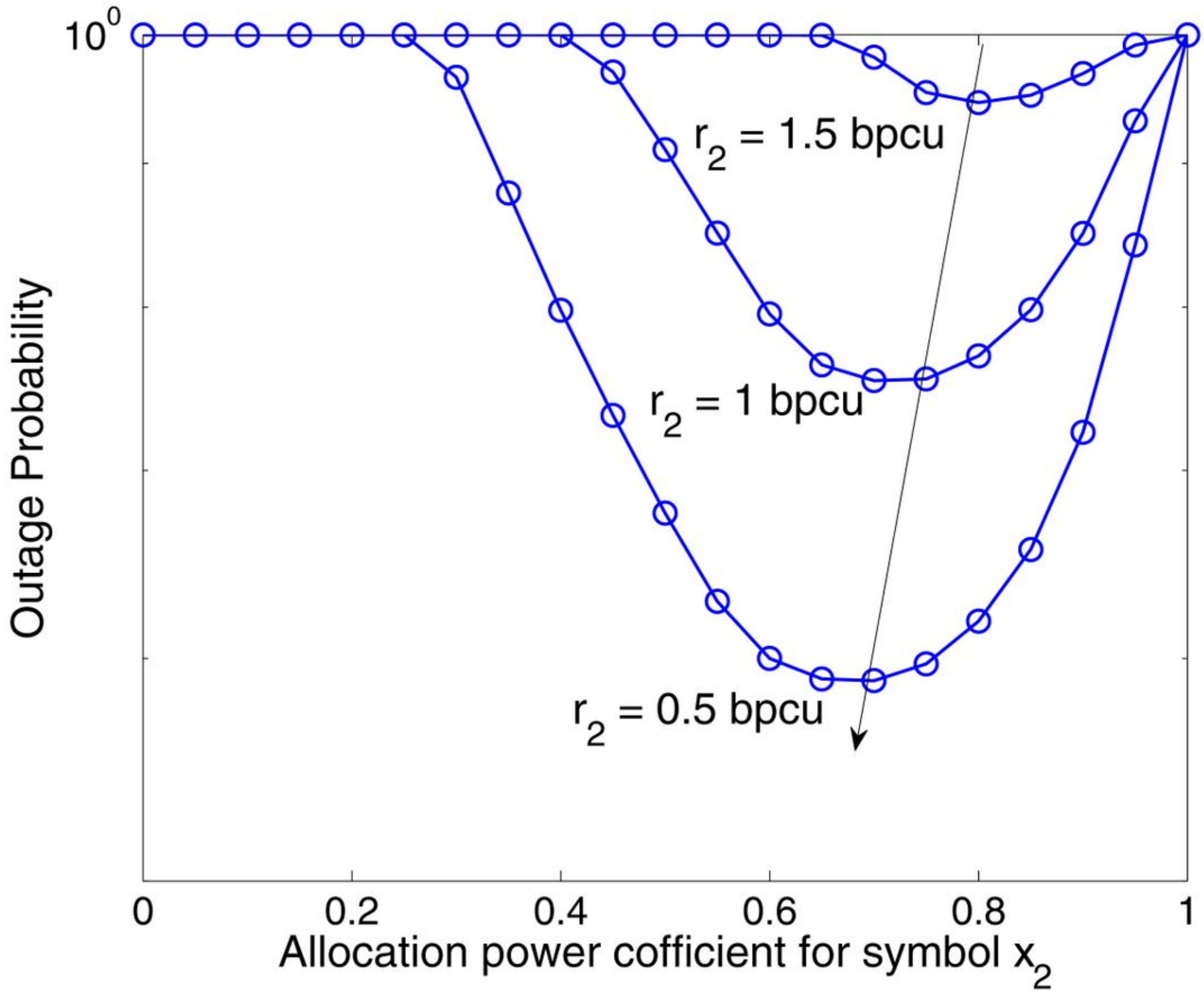

Figure 8

The effect of power allocation coefficient on the OP for different data rates, EbNo = 10dB.

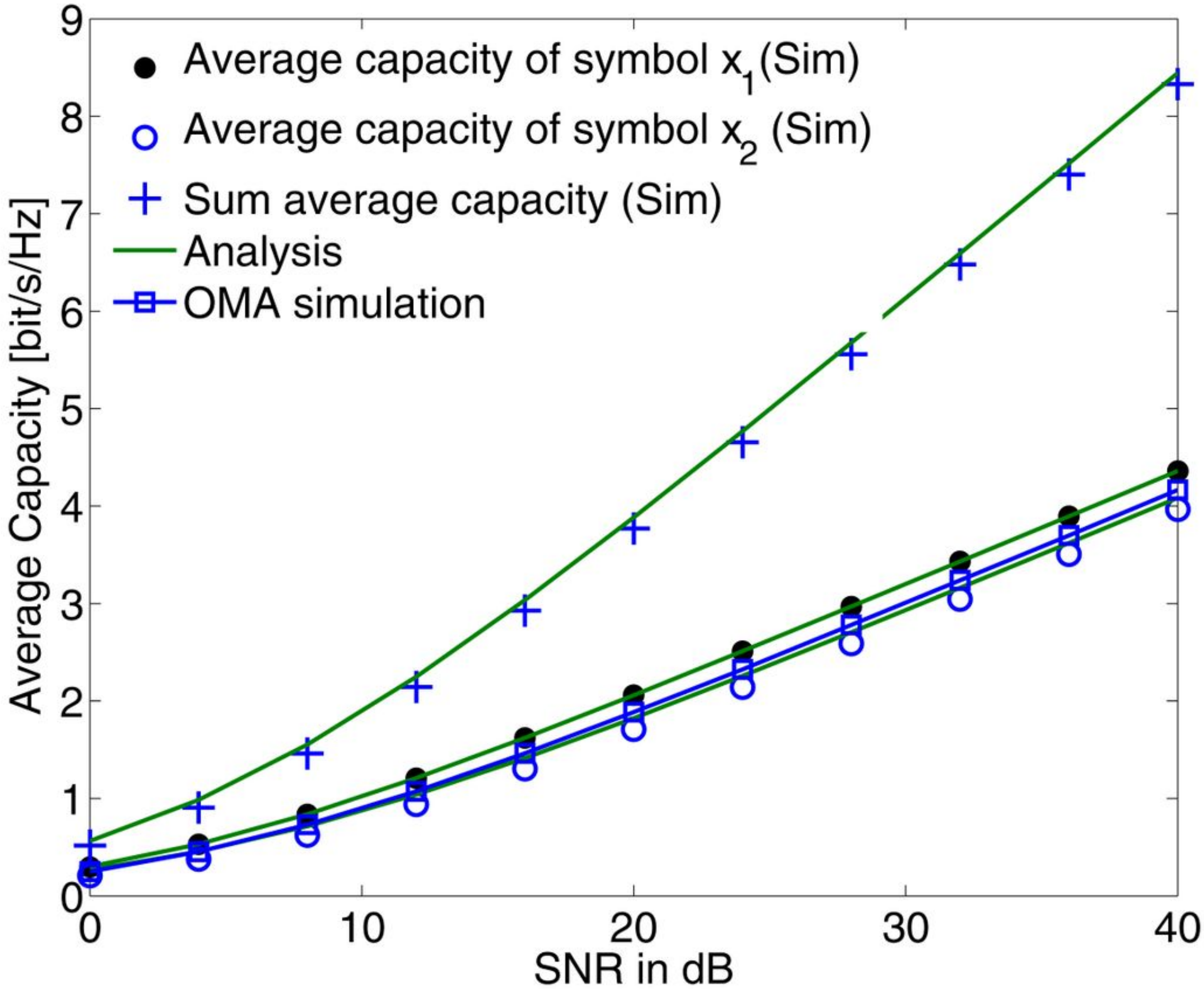

Figure 9

Average capacity of the system versus its SNR.